WL-TR-89-29

DTIC FILE COPY

AD-A213 082

# GENERATION OF IODINE MONOFLUORIDE IN A SUPERSONIC MULTIPURPOSE FLOWTUBE FACILITY

Charles A. Helms

August 1989

DTIC
ELECTE
OCT 0 2 1989
S D
D

Final Report

Approved for public release; distribution unlimited.

WEAPONS LABORATORY
Air Force Systems Command
Kirtland Air Force Base, NM 87117-6008

89 10 2 055

This final report was prepared by the Weapons Laboratory, Kirtland Air Force Base, New Mexico, Job Order 33260385. Leonard Hanko (ARDI) was the Laboratory Project Officer-in-Charge.

When Government drawings, specifications, or other data are used for any purpose other than in connection with a definitely Government-related procurement, the United States Government incurs no responsibility or any obligation whatsoever. The fact that the Government may have formulated or in any way supplied the said drawings, specifications, or other data, is not to be regarded by implication, or otherwise in any manner construed, as licensing the holder, or any other person or corporation; or as conveying any rights or permission to manufacture, use, or sell any patented invention that may in any way be related thereto.

This report has been authored by employees of the United States Government. Accordingly, the United States Government retains a nonexclusive, royalty-free license to publish or reproduce the material contained herein, or allow others to do so, for the United States Government purposes.

This report has been reviewed by the Public Affairs Office and is releasable to the National Technical Information Service (NTIS). At NTIS, it will be available to the general public, including foreign nationals.

If your address has changed, if you wish to be removed from our mailing list, or if your organization no longer employs the addressee, please notify WL/ARDI, Kirtland AFB, NM 87117-6008 to help us maintain a current mailing list.

This report has been reviewed and is approved for publication.

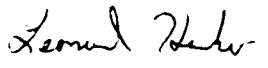

LEONARD HANKO
Project Officer

FOR THE COMMANDER

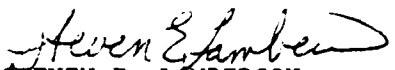

STEVEN E. LAMBERSON
Major, USAF
Chief, Advanced Chemical Laser Branch

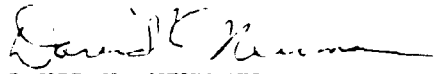

DAVID K. NEUMANN
Major, USAF
Chief, Devices Division

DO NOT RETURN COPIES OF THIS REPORT UNLESS CONTRACTUAL OBLIGATIONS OR NOTICE ON A SPECIFIC DOCUMENT REQUIRES THAT IT BE RETURNED.

UNCLASSIFIED
SECURITY CLASSIFICATION OF THIS PAGE

# REPORT DOCUMENTATION PAGE

Form Approved
OMB No 0704-0188

| | |
|---|---|
| 1a REPORT SECURITY CLASSIFICATION<br>Unclassified | 1b RESTRICTIVE MARKINGS |
| 2a. SECURITY CLASSIFICATION AUTHORITY | 3 DISTRIBUTION / AVAILABILITY OF REPORT<br>Approved for public release; distribution unlimited. |
| 2b. DECLASSIFICATION / DOWNGRADING SCHEDULE | |
| 4. PERFORMING ORGANIZATION REPORT NUMBER(S)<br>WL-TR-89-29 | 5. MONITORING ORGANIZATION REPORT NUMBER(S) |
| 6a. NAME OF PERFORMING ORGANIZATION<br>Weapons Laboratory<br>6b. OFFICE SYMBOL (If applicable)<br>ARDI | 7a. NAME OF MONITORING ORGANIZATION |
| 6c. ADDRESS (City, State, and ZIP Code)<br>Kirtland Air Force Base,<br>New Mexico 87117-6008 | 7b. ADDRESS (City, State, and ZIP Code) |
| 8a. NAME OF FUNDING / SPONSORING ORGANIZATION<br>8b OFFICE SYMBOL (If applicable) | 9 PROCUREMENT INSTRUMENT IDENTIFICATION NUMBER |
| 8c. ADDRESS (City, State, and ZIP Code) | 10 SOURCE OF FUNDING NUMBERS |

| PROGRAM ELEMENT NO | PROJECT NO | TASK NO | WORK UNIT ACCESSION NO |
|---|---|---|---|
| 62601F | 3326 | 03 | 85 |

11. TITLE (Include Security Classification)
GENERATION OF IODINE MONOFLUORIDE IN A SUPERSONIC MULTIPURPOSE FLOWTUBE FACILITY

12. PERSONAL AUTHOR(S)
Helms, C. A.; Hanko, L.; Miller, J.; Healey, K.P.; Hager, G.; and Perram, G.P.

| 13a. TYPE OF REPORT | 13b. TIME COVERED | 14. DATE OF REPORT (Year, Month, Day) | 15. PAGE COUNT |
|---|---|---|---|
| Final | FROM May 88 TO Oct 88 | 1989, August | 54 |

16. SUPPLEMENTARY NOTATION

| 17. COSATI CODES | | |
|---|---|---|
| FIELD | GROUP | SUB-GROUP |
| 07 | 02 | |
| | | |

18. SUBJECT TERMS (Continue on reverse if necessary and identify by block number)
Iodine Monofluoride
Nitrosyl Fluoride
Visible Chemical Laser
Nitric Oxide
Fluorine

19. ABSTRACT (Continue on reverse if necessary and identify by block number)
Iodine monofluoride, a promising visible chemical laser candidate, has been chemically produced at number densities exceeding $1x10^{15}$ molecules/$cm^3$ in a supersonic flow. The low pressure (3 torr), low temperature (300 K) flow environment should be suitable for lasing.

| 20. DISTRIBUTION / AVAILABILITY OF ABSTRACT | 21. ABSTRACT SECURITY CLASSIFICATION |
|---|---|
| ☐ UNCLASSIFIED/UNLIMITED ☐ SAME AS RPT ☒ DTIC USERS | Unclassified |

| 22a. NAME OF RESPONSIBLE INDIVIDUAL | 22b. TELEPHONE (Include Area Code) | 22c. OFFICE SYMBOL |
|---|---|---|
| Charles A. Helms | (505) 844-0661 | WL/ARDI |

DD Form 1473, JUN 86 Previous editions are obsolete.



SECURITY CLASSIFICATION OF THIS PAGE
UNCLASSIFIED

CONTENTS





Accesion For
NTIS CRA&I
DTIC TAB
Unannounced
Justification
By
Distribution /
Availability Codes
Dist
A-1

CONTENTS (CONCLUDED)

FIGURES

FIGURES (CONCLUDED)

# 1.0 INTRODUCTION

The idea of constructing a multipurpose test-bed for small-scale flowtube experiments was conceived several years ago. The anticipated uses of such a device have evolved since that time into two principal themes. One is the advancement of COIL (chemical oxygen-iodine laser) technology, including flow characteristics, determining rate constants, and developing new optical diagnostic tools. The other stated purpose of the flowtube is to pursue the development of a visible chemically pumped laser system. It is toward the latter objective that the work described herein was directed.

The development of a chemically pumped, short-wavelength laser has been pursued for the last 15 yr. Despite these vigorous efforts, there has been no clear demonstration of such a system (Ref. 1). The task is difficult because of several factors, including: (1) the high density of states accessible by extremely exothermic reactions, (2) a strong dependence of radiative transition probability on frequency, (3) difficult preparation of reagents, and (4) complex reactive mixing requirements. The last two issues are addressed in the present study.

One approach to demonstrating a visible chemical laser is through energy transfer schemes analogous to that employed by COIL (Ref. 2). A metastable energy carrier is selectively produced under the constraint of spin conservation and this stored energy is kinetically transferred to a suitable lasing molecule. A promising candidate for an energy acceptor in a visible chemical laser is the iodine monofluoride (IF) molecule. The characteristics of the IF $B^3\Pi(0^+) \rightarrow X^1\Sigma(0^+)$ (IF(B→X)) system that make it attractive as a potential lasing specie are numerous and have been discussed in detail elsewhere (Refs. 3,4). A continuous-wave, optically pumped IF laser has been demonstrated which operates between the vibrationally thermalized levels of $B^3\Pi(0^+)$ and the high vibrational levels ($v''$ = 7-11) of $X^1\Sigma(0^+)$ (Ref. 3). Also, a considerable body of work exists which examines potential energy donor partners for IF (Refs. 4-6). Iodine monofluoride is not a stable molecule, surviving only a few milliseconds in environments common to flowing gas phase laser systems

(Ref. 7). This constraint requires real time in situ production of ground state IF (IF(X)), usually by combining molecular iodine ($I_2$) with atomic fluorine (F) or molecular fluorine ($F_2$). One major obstacle in demonstrating a chemically pumped IF(B→X) laser has been the production of sufficient number densities of IF(X). For example, it has been estimated that $\approx 10^{15}$ molecules/cm$^3$ IF(X) would be required to lase IF(B→X) in a $O_2(^1\Delta)$ pumped laser scheme (Ref. 8). The maximum number densities previously reported have been on the order of $10^{13}$ molecules/cm$^3$ (Refs. 3 and 9).* A method for generating IF(X) number densities in excess of $1\times10^{15}$ molecules/cm$^3$ using the F + $I_2$ reaction is presented here. The key step is the production of high number densities of fluorine atoms, which then react with $I_2$ at a gas kinetic rate. The combustion of NO with $F_2$ has previously been used to produce fluorine atoms for hydrogen fluoride (HF) chemical lasers (Ref. 10), and was chosen as the fluorine atom source in the present study.

---

*References 3 and 9 assumed $10^{15}$/cm$^3$ IF(X) based on the $I_2$ delivery. In Reference 8, Davis, et al directly measured IF(X) absorption and determined the number density to be only $10^{13}$/cm$^3$.

# 2.0 FACILITY

## 2.1 OVERVIEW

This section describes all of the systems which constitute the flowtube facility, located in Building 617 at Kirtland Air Force Base in Albuquerque, New Mexico.

A schematic representation of the flowtube facility is shown in Fig. 1. The facility has been divided into several component blocks which are discussed individually. The device consisted of a supersonic nozzle through which gases flowed from storage bottles to a pump system. The gases reacted in the device. Optical and medium (temperature and pressure) diagnostics were used to monitor the device's performance (Figs. 2,3).

The flowtube itself was situated over a 5- by 12-ft optical table to facilitate optical measurements. The pump system was housed in a separate utility building immediately adjacent to the main building. Overhead cable trays were used to house cabling between the device and the control room. A 3000 $ft^3$/min ceiling fan was located directly over the flowtube to aid in venting the room in the event of a gas leak. The device was enclosed in 0.125-in Plexiglas shields to contain gas leaks.

This section is meant only to give a feel for the physical setup of the flowtube device. More detailed information is given in the Appendix.

## 2.2 FLUID SUPPLY SYSTEM

### 2.2.1 General Information

2.2.1.1 Mass Flow Controllers. All gas flows were controlled with calibrated mass flow controllers (Unit Mfg. model UFC-3020). Although each controller was calibrated for a specific gas, manufacturer-supplied correction factors allowed any gas to be used. The controllers were capable of metering up to 100 standard l/min and were rated accurate to ±1 percent of full scale.

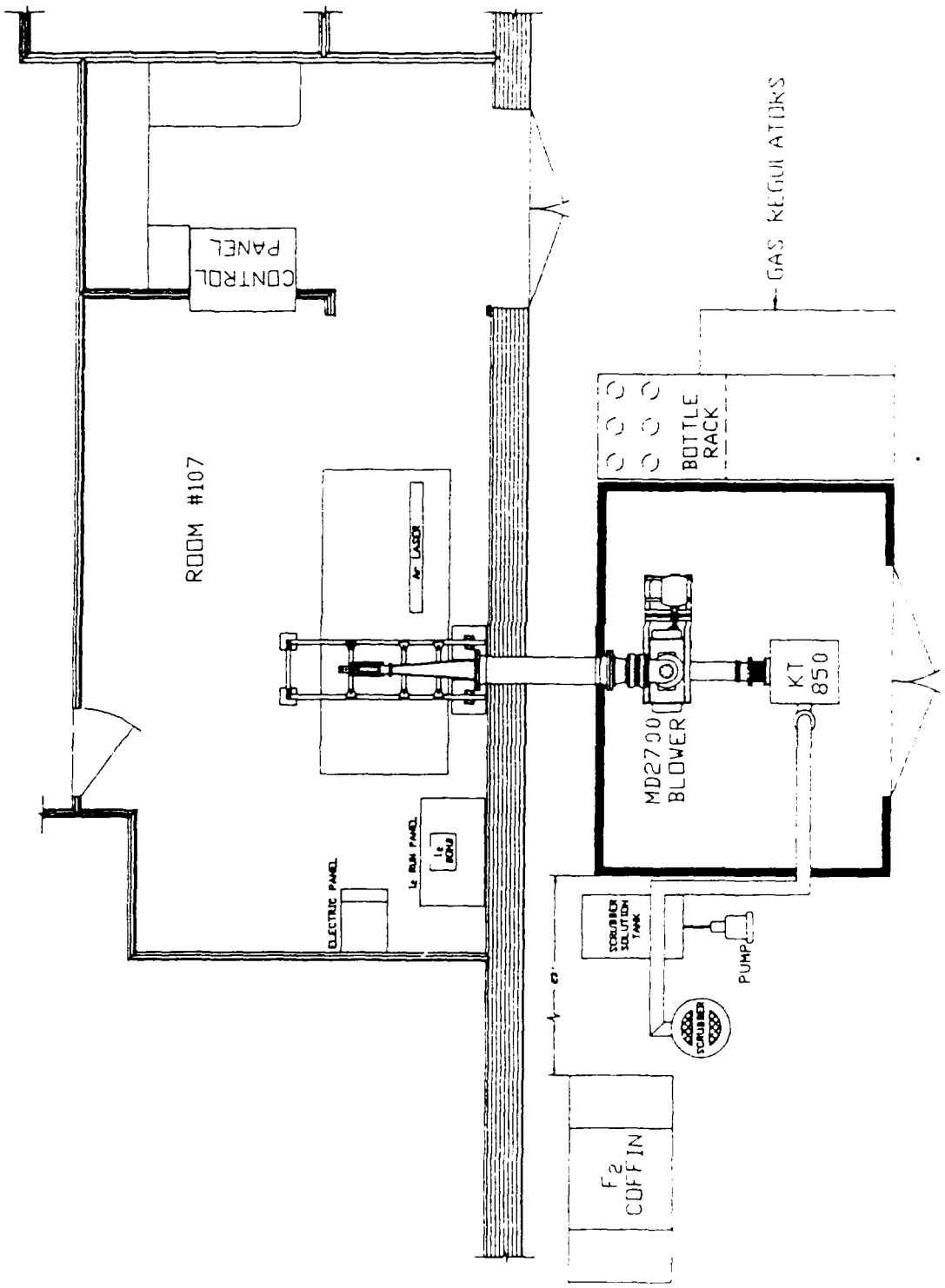


Figure 1. Schematic view of entire flowtube facility

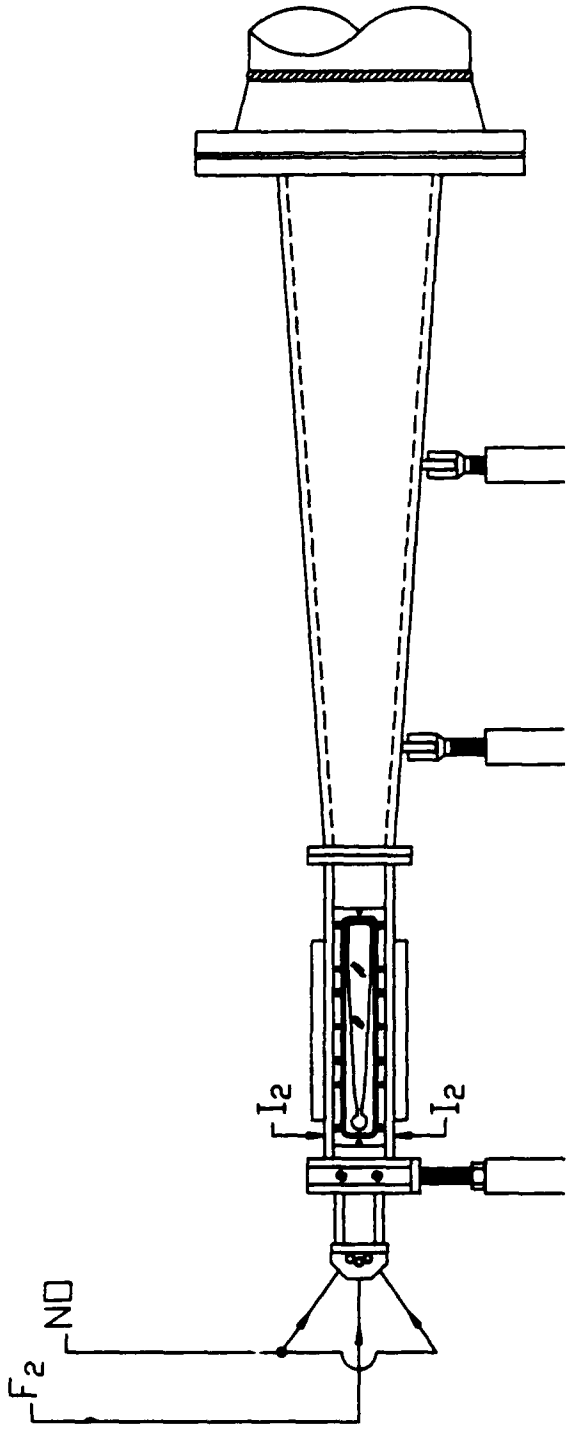


Figure 2. Schematic illustration of the flowtube device.

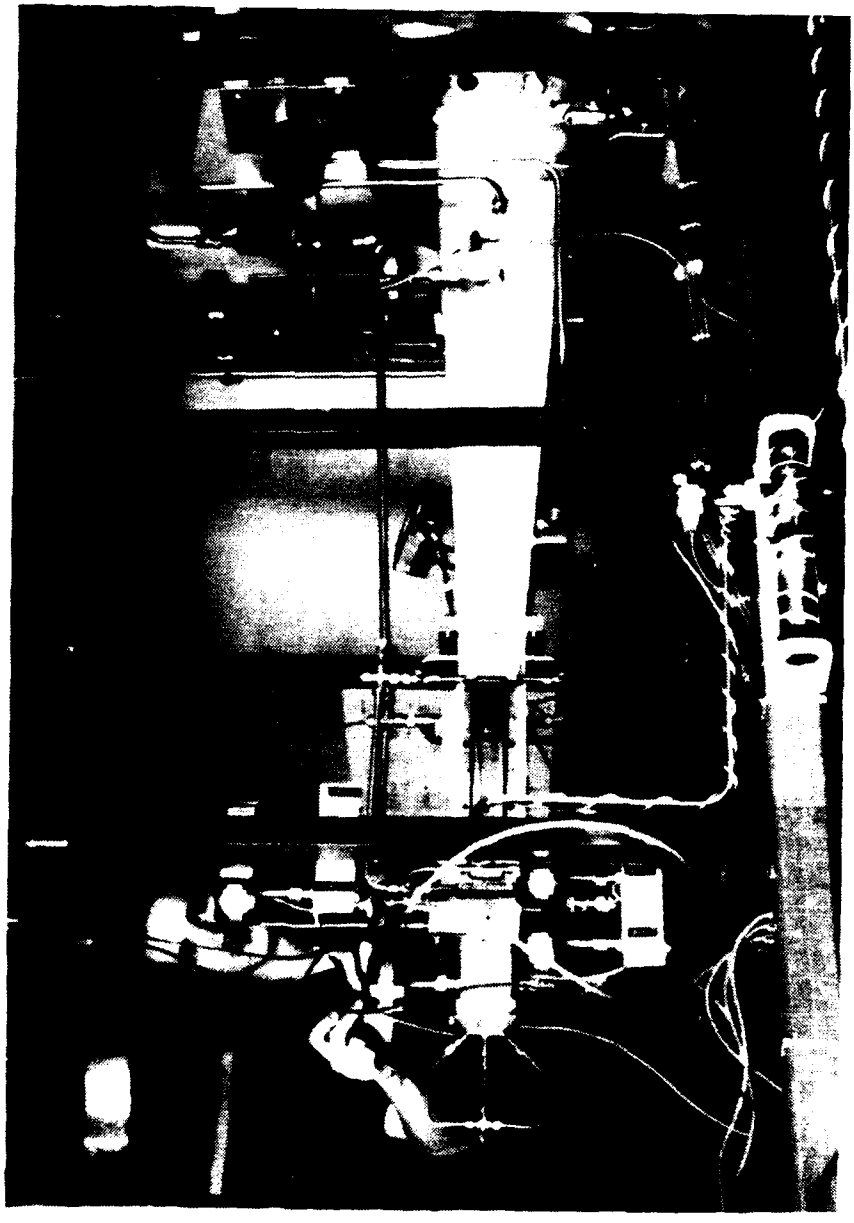

Figure 3. Photograph of flowtube.

2.2.1.2 Gas Detectors. Nitric oxide, $F_2$, and $I_2$ are toxic substances whose gas phase concentrations must be continually monitored. Commercially made gas detection/warning systems were used for each gas. Table 1 gives the pertinent information concerning the gas detectors.

TABLE 1. Warning and alarm settings of gas detectors.

| GAS | MANUFACTURER | WARNING SETTING(ppm) | ALARM SETTING(ppm) | TLV* (ppm) | IDLH** (ppm) |
|---|---|---|---|---|---|
| nitric oxide | Enterra (model 5102) | 10 | 25 | 25 | 100 |
| fluorine | Enterra (model 5152-E) | 0.5 | 2 | 0.1 | 25 |
| iodine | Mast (model 1724) | none | 1 | 0.1 | 25 |

*TLV is the 40 hr/wk exposure limit set by the Occupation Safety and Health Administration (OSHA).

**IDLH is the maximum level that can be tolerated for 30 min without irreversible damage, as established by OSHA.

Two NO sensors were employed; one on the device and another between the device and the control panel. Because of the extreme danger presented by NO, which is odorless and colorless, the NO detectors were tested on each run day. This was done by exposing the sensors to 30 ppm of NO in air from a pressurized bottle obtained from Scientific Industries Inc.

2.2.1.3 Diluents. Nitrogen ($N_2$), argon (Ar), and helium (He) were used to dilute the reactive gases prior to injection into the device. Nitrogen and He were supplied by permanent facility plumbing. Argon was supplied by four standard K-bottles manifolded together. The plumbing design required that once a diluent gas was selected for a given run, that gas had to be used as the diluent throughout the device. The device could be modified to accept a different diluent gas in < 10 min.

### 2.2.2 Fluorine System

Fluorine was obtained in standard 400 lb/in$^2$ K-bottle cylinders and stored on site in a 4- by 4- by 7-ft steel coffin. One-half inch stainless steel lines were used to transport the fluorine to the device. The lines were passivated prior to use by trapping increasing fluorine concentrations in the lines for several hours each. Diluent was added to the fluorine flow just outside the fluorine containment coffin to minimize the length of line exposed to pure fluorine. Fluorine and diluent flows were enabled by remotely actuated valves and controlled by calibrated mass flow controllers. A thin insulated wire (fleek wire) was wrapped around all fluorine lines which would abort the entire system if broken by, for example, a fluorine fire.

### 2.2.3 Nitric Oxide System

Nitric oxide also was obtained in 400 lb/in$^2$ K-bottles, which were stored outside. The NO was delivered to the device by 0.5-in stainless steel lines. Diluent was mixed into the NO before entering the building. The NO line was split into two lines for injection at two points in the combustor (see Section 2.3.1).

### 2.2.4 Iodine System

Gas phase $I_2$ was delivered from a heated sublimation bed (6-in in diameter and 18-in long) by flowing 30 to 70 mmol/s of preheated diluent over the bed (Fig. 4). The $I_2$ diluent flow was split prior to metering so that known flows of diluent could be passed around the bed as well as through it. This allowed both the desired amount of $I_2$ to be extracted from the bed and the total flow to be varied to ensure penetration of the $I_2$ flow into the combustor effluent. The diluent flow through the bed was diverted to an alternate path until an $I_2$ flow was desired. The bed was half filled with solid $I_2$ and heated to 80 to 110°C with two 550-W quartz rod heaters. The liberated $I_2$ (1.0-3.0 mmol/s) was injected into the combustor exit flow $\approx$ 1.0 cm upstream of the choking throat at the combustor exit. All lines

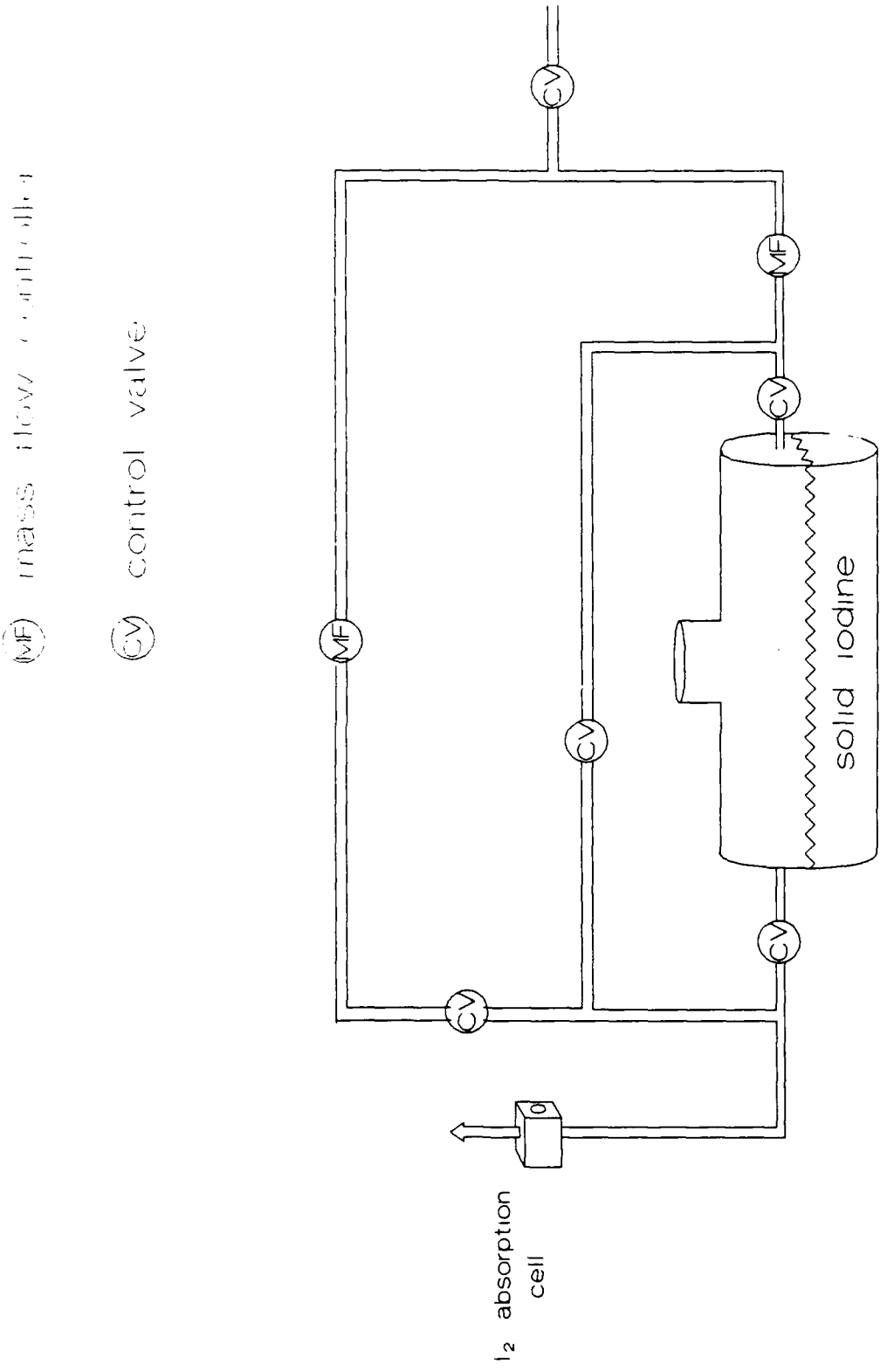


Figure 4. Iodine system layout.

associated with the $I_2$ system were heated to 120 to 150°C to prevent coating the inner surface of the lines with $I_2$.

## 2.3 DEVICE HARDWARE

The hardware described in this section was designed and fabricated locally. Stainless steel was used for all components except the windows which were made from Plexiglas. For more detailed information refer to the drawings listed in Table 2.

TABLE 2. Drawing numbers of final flowtube drawings.

| drawing name | Rockwell drawing number |
|---|---|
| layout, coil diagnostic flowtube | 8716382 |
| layout, combustor | 8716383 |
| combustor manifold* | 8716384 |
| housing, combustor | 8716385 |
| optional combustor blade* | 8716386 |
| spacer* | 8716387 |
| housing* | 8716388 |
| ramp-entrance | 8716389 |
| nozzle | 8716390 |
| nozzle blade* | 8716391 |
| plate - side inr | 8716392 |
| outer side plate* | 8716393 |
| window-upr,lwr | 8716394 |
| window-side | 8716395 |
| diffuser, coil diag. flowtube | 8716397 |
| assembly, I2 bomb IF | 8816004 |
| IF, fluid supply system schematic* | 62IFE001 |

*shown in Appendix

### 2.3.1 Combustor

The $NO\backslash F_2$ combustor consisted of two main components, the injector manifold and the combustor body (Fig. 5). A triplet injector was used to introduce the NO and $F_2$ into the combustor. The NO flow was split and injected from the top and bottom, while the fluorine was injected in the middle. The NO injectors each consisted of a row of 20 holes 0.023 in in diameter. The fluorine injector had 21 holes of 0.032-in diameter. The combustor was 2-in wide and 8-in long from the $NO\backslash F_2$ injectors to the iodine injectors. The height was 2.0 cm for approximately the first 4 in and decreased to 0.25 in previous to iodine injection.

Provision was made for an additional throat to be installed roughly at the halfway point of the combustor. The throat consisted of two symmetric pieces bolted onto the inner walls of the combustor with a 0.048-in horizontal slit between them.

### 2.3.2 Iodine Injectors

Iodine was injected into the device symmetrically from the top and bottom (Fig. 5). Each injector consisted of two rows of 42 0.032- and 0.016-in diameter holes normal to the flow direction (Fig. 6). The injector blocks were heated with 0.25-in diameter 150-W cartridge heaters to prevent clogging the holes with solid $I_2$.

### 2.3.3 Nozzle Assembly

The nozzle assembly consisted of the main choking throat, gas expansion ramps, window purges, and Plexiglas windows (Fig. 5). An inner section containing the throat and ramps slid into an outer housing mounted to the downstream side of the device (diffuser section). Window purge plates bolted to the housing from the outside. The throat was produced by narrowing the vertical dimension of the combustor exit from 0.25 to 0.2-in with the upstream edges of the expansion ramps.

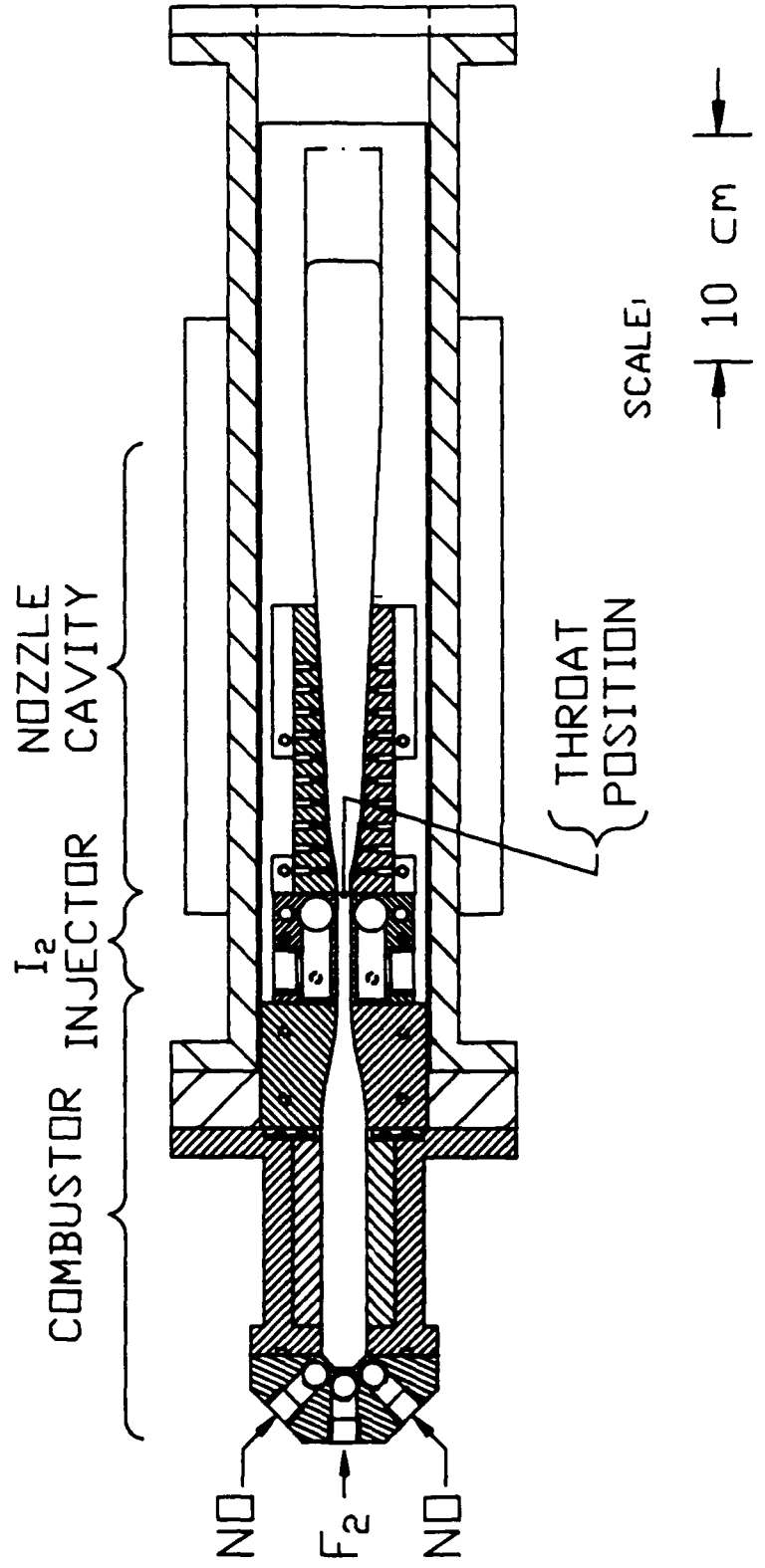


Figure 5. The NO\$F_2$ combustor and nozzle assembly.

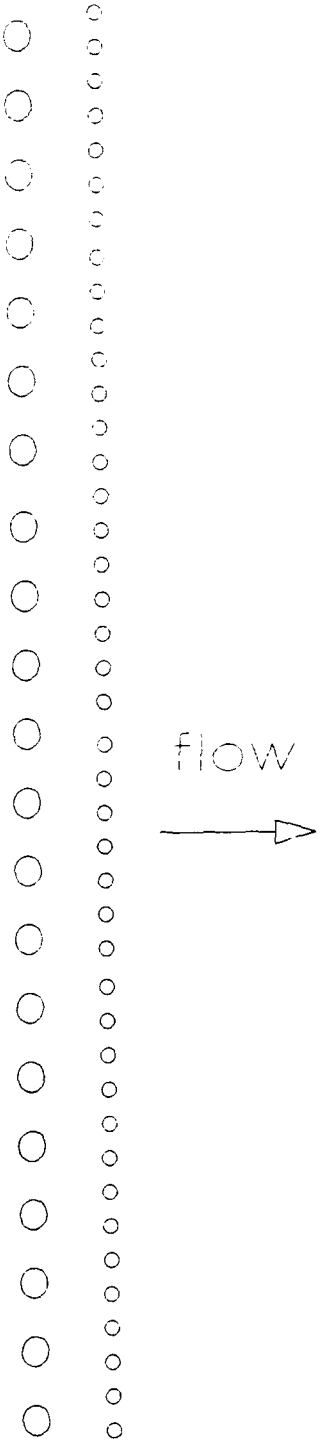


Figure 6. Iodine injector hole pattern.

## 2.4 PUMP SYSTEM

The device was evacuated with a Kinney model KT850 single-stage rotary pump assisted by a Roots model MD2700 blower which together provided a total pumping capacity of roughly 1100 *l*/s. The device was pumped down from ambient pressure through a 0.5-in line to avoid shocking the pump. The main vacuum valve (10 in) was opened once the device pressure was below 100 torr, and the blower was activated after the pressure dropped below 10 torr. The lowest pressure attainable in the flowtube with all flows off was 10 mtorr. This pressure was measured with a thermocouple gauge calibrated with a diffusion pump system. The leak rate in the device was 0.3 to 0.4 torr/min. This corresponds to a leak flow rate of < 1 percent of the nominal fluorine flow rate.

The pump exhaust was passed through a 20-ft vertical pipe filled with 1.5-in diameter plastic spheres. A 20 percent sodium hydroxide (NaOH) solution was continuously pumped into the top of the 12-in diameter pipe to coat the spheres. This solution has been effective in removing harmful compounds from the pump's exhaust.

## 2.5 TEMPERATURE AND PRESSURE MEASUREMENTS

Temperatures were measured with T type thermocouples. Gas-phase thermocouples were used in the iodine cell and the combustor. Figure 7 shows the positions of all thermocouples on the device.

Baratron pressure transducers with ranges of 0 to 10, 0 to 100, and 0 to -1000 torr were used to monitor pressures. Figure 7 shows the positions of all the pressure transducers on the device. Fluorine compatible transducers (such as Dynisco) must be used for the fluorine plenum.

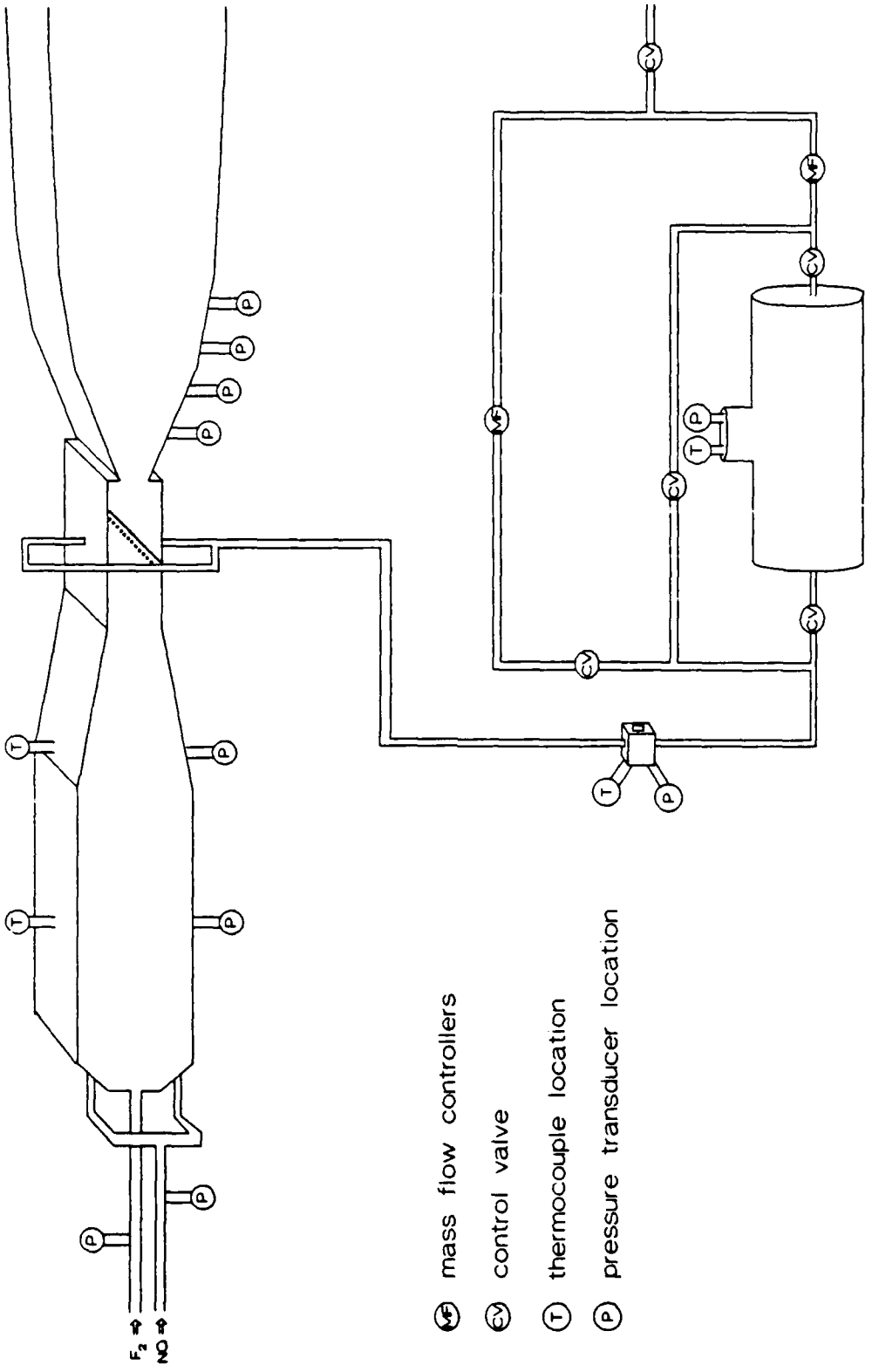


Figure 7. Location of all thermocouples and pressure transducers on the flowtube.

## 2.6 CONTROL PANEL

### 2.6.1 Separate Subsystems

The control panel was configured in separate subpanels, each consisting of six rocker switches (Fig. 8). The panel contained 12 of these modular, interchangeable units. The experiments described herein required five of the subpanels for $F_2$, NO, $I_2$, the pump system, and the device.

### 2.6.2 System Aborts

The control panel had separate momentary switches to activate each subpanel, and another set to abort each subpanel. There was also a main activation switch and a system abort that closed all valves simultaneously. As mentioned previously (Section 2.2.2), a burn-through of fleek wire on the fluorine lines would abort the system.

### 2.6.3 Panel Power Sources

The panel was powered by a 30-V power supply connected to the facility. Two car batteries connected in series served as backup power, which automatically came on-line in the event of main power loss. A battery charger was also in the circuit to maintain the charge on the batteries. The panel contained indicator lights to inform the operator which power source was being used.

## 2.7 DATA ACQUISITION AND PROCESSING

### 2.7.1 Computer Interface

All of the diagnostic signals were interfaced to the acquisition computer via analog-to-digital (A/D) interface cards. Thermocouple signals were amplified by Omega thermocouple conditioning units. The temperature, pressure, and mass flow signals passed through a Data Translation 2806 A/D card, which can handle up to 48 0- to 5-V signals. Two Data Translation 2821 A/D cards provided a total of 32 0- to 10-V channels that were used

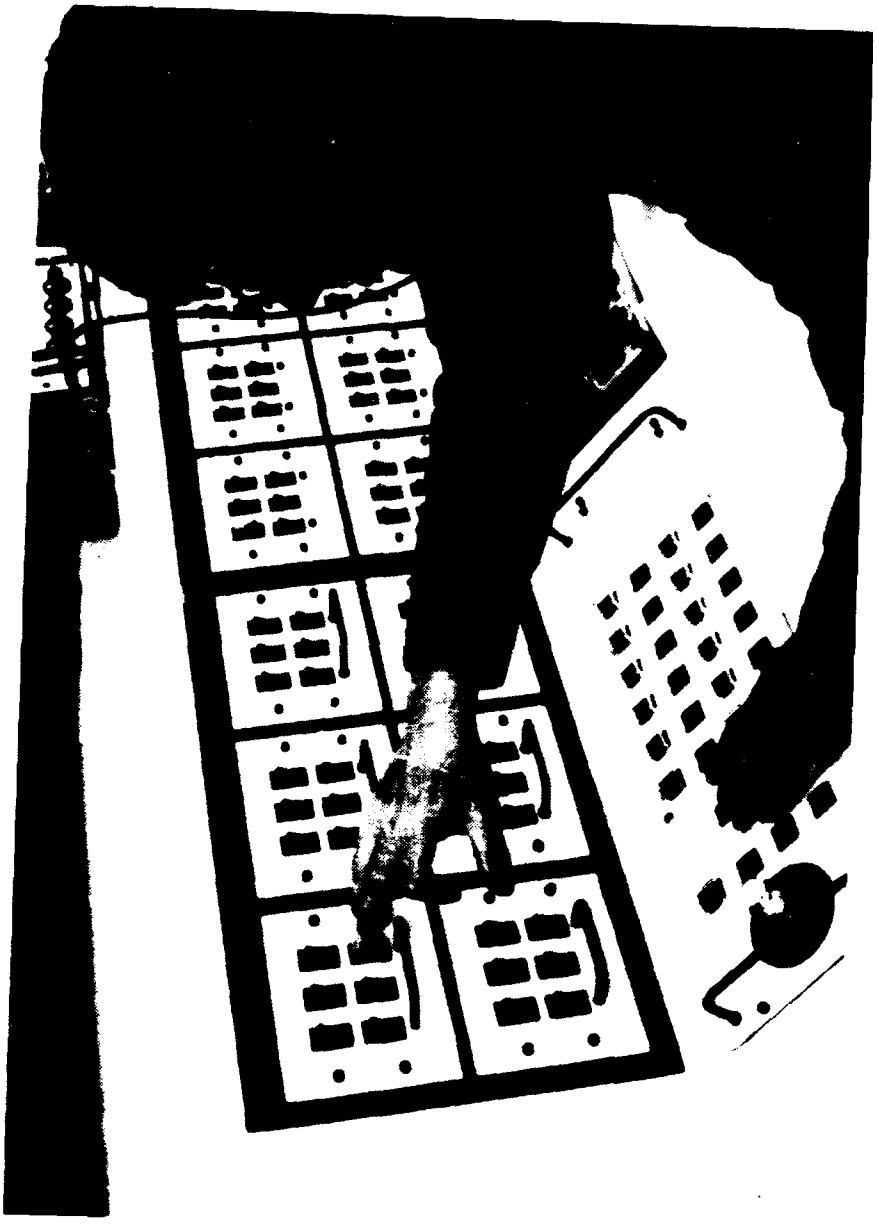

Figure 8. Photograph of control panel.

for optical diagnostics. For the IF experiments, 11 pressures, 12 temperatures, and 8 mass flows were connected to the 2806 card and 4 to 7 signals were connected to the 2821 cards. All inputs were single-ended.

### 2.7.2 Acquisition Software

Data acquisition was handled by an IBM AT clone equipped with 20 and 30 megabyte hard disks and 2.5 Mbyte of random access memory (RAM). The acquisition software was written in the C computer language. The code was designed to run continuously, providing the operator with four separate screens of current diagnostic information in both raw (voltage) and processed (engineering units) form. The A/D channels could be scanned at rates of 1, 2, 5, 10, and 20 Hz. The screen display routine ran continuously and was interrupted to sample data at the desired rate. Data were written to RAM in real time and transferred to 1.2 Mbyte flexible disks after each run. A 10-s background was collected immediately before each run, and this information was used to interpret run-time data. A calibration file containing the interpretation of each A/D channel and relevant scale factors also was generated for each run. These files were then transferred on disk to the reduction machine for processing.

### 2.7.3 Reduction Software

A Zenith model ZFX-0248-50 microcomputer was used for data reduction and analysis. The reduction code was written in a menu driven format, and was also in the C language. A halo-graphics driver was used to plot both raw and processed (engineering units) data on the screen. Up to six sensor readings could be plotted at a time. Hard copies of plots were available as screen dumps onto a Hewlett Packard Laserjet printer. The code could also compute average values for each sensor over a user selected time frame. This feature was used extensively. The raw data were permanently stored on 1.2 Mbyte flexible disks and on magnetic tape.

## 2.8 GENERAL OPERATING INFORMATION

Each device test (or run) took about 1 min. Ten to 20 tests were conducted per day. Over 300 tests were conducted on 25 test days over a 3-mo period. A typical test consisted of (1) beginning data acquisition, (2) turning on the iodine at 10 s, (3) turning on the combustor at 25 s, (4) turning off the combustor at 50 s, (5) turning off the iodine at 60 s, and (6) ending data acquisition at 70 s.

Typical flow rates are given in Table 3. Combustor pressure without the additional throat was ≈ 20 to 30 torr. The pressure in the nozzle cavity, where most of the optical diagnostic measurements were made, was only 2 to 4 torr. Typical gas-phase temperatures ranged from room temperature in the cavity to 600 K in the combustor.

TABLE 3. Typical flow rates in flowtube.

| GAS | NOMINAL FLOW RATE (mmoles/s) |
|---|---|
| fluorine | 7 |
| fluorine diluent | 17.5 |
| nitric oxide | 7 |
| nitric oxide diluent | 17.5 |
| iodine | 2 |
| iodine diluent (run) | 50 |
| iodine diluent (bypass) | 10 |
| window purge | 15 |

## 3.0 OPTICAL DIAGNOSTICS

Iodine delivery was monitored by continuum absorption at 488 nm using a Coherent model CR8 argon ion laser.* Iodine absorption was measured in a diagnostic cell (2.5-cm optical path) prior to injection (Fig. 9) and in the nozzle expansion section after injection (Fig. 10). The IF(X) concentration in the nozzle was measured by absorption with a Coherent model 699-29 ring dye laser pumped by a Coherent model CR3000K krypton ion laser operated multiline in the violet (Fig. 11). A Burleigh WA-20 wavemeter was used to monitor the frequency of the ring laser during laser sweeps (~1 $cm^{-1}$). The bandwidth of the ring laser was determined to be <100 MHz with a Tropel model 360 interferometer. Diagnostic beams were passed through the 5-cm effective path of the cavity 1 to 7 times (in a vertical plane normal to the flow) to increase absorption as desired. Isentropic flow calculations predict flow velocities of Mach 2 to 3 in the cavity. Thus, the beam diameters of ≈2 mm yield a temporal resolution of ≈ 3 $\mu$s. Emission in the cavity was monitored by either a RCA 4836 PMT (equipped with a 6000 Å long pass filter) or dispersed through a 0.3-m McPherson polychromator and onto an EG&G 1024 element optical multichannel analyzer. Penetration of the iodine jets into the combustor exit flow was checked by pumping $I_2(X \rightarrow B)$ with a telescoped $Ar^+$ laser operated at 5145 Å and observing $I_2(B \rightarrow X)$ emission. The $I_2$ was fully penetrated, even at low $I_2$ diluent flow rates.

The ring laser absorption measurement was checked for saturation by varying the power from 0.1 to 4.0 mW and the path length from 5 to 35 cm. No effect on the calculated number densities was observed.

---

*Davis, S.J. et al "Halogen Mass Flow Rate Detection System", patent no. 4,467,474 1984.

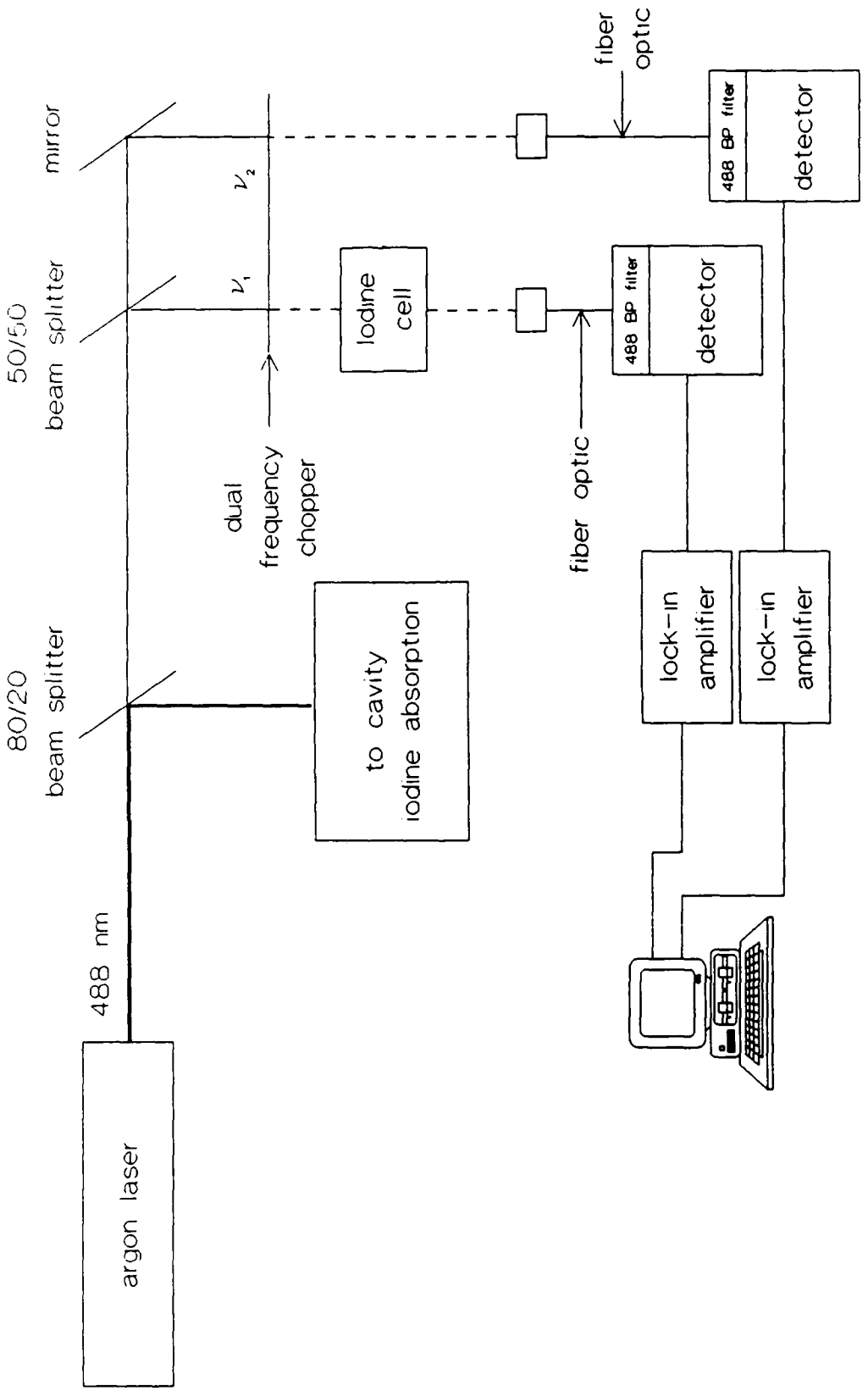


Figure 9. Schematic illustration of iodine absorption diagnostic in the iodine diagnostic cell.

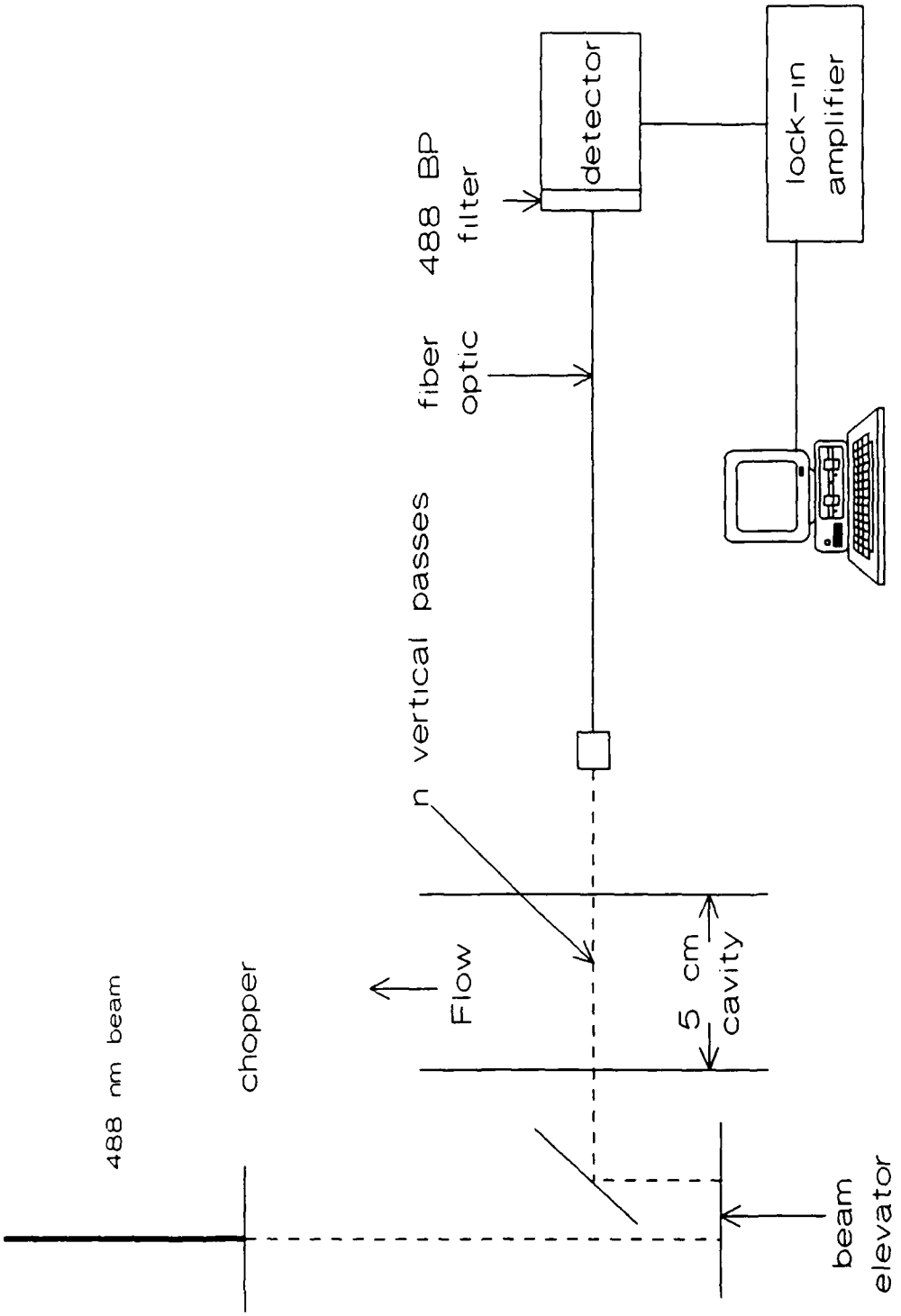


Figure 10. Schematic illustration of iodine absorption diagnostic in the flowtube cavity.

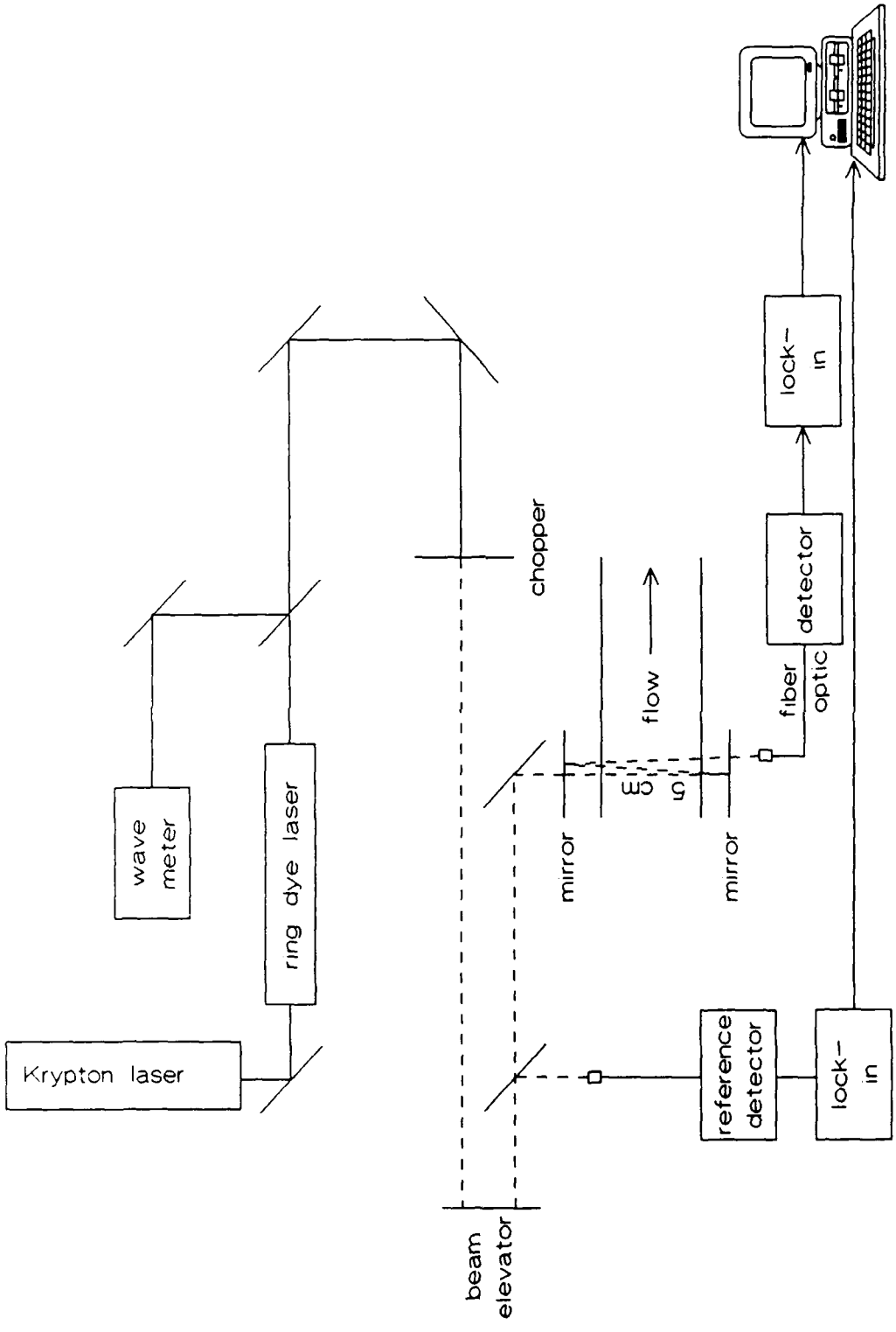


Figure 11. Schematic illustration of IF absorption diagnostic in the flowtube cavity.

# 4.0 RESULTS

## 4.1 IODINE REMOVAL

The diagnostic first used to infer IF(X) production was the consumption of $I_2$ in the nozzle cavity, presumably from the F + $I_2$ reaction. Figure 12 shows a typical $I_2$ concentration time profile in the nozzle cavity. During this run $I_2$ flowed through the cavity from t = 11 to t = 48 s, whereas the F atom generator was on from t = 22 to t = 36 s. The decrease in the $I_2$ absorption while the combustor was activated was used to calculate the $I_2$ removal.

## 4.2 IODINE MONOFLUORIDE PRODUCTION

Direct absorption by IF(X) was used to verify the $I_2$ removal results. Rotational lines of the IF(X,$v'' = 0 \rightarrow v' = 5$) vibrational band were used because of their favorable Franck-Condon factors. No absorption was observed from $v'' = 1$. In light of the detection limit for $v'' = 1$ ($6 \times 10^{13}$ molecules/$cm^3$), this is consistent with a room temperature Boltzmann vibrational distribution ($v'' = 1/v'' = 0 = 0.05$). A ring dye laser absorption scan of the R(33) and P(26) rotational lines of the IF($v'' = 0 \rightarrow$ B, $v' = 5$) band is shown in Fig. 13. The rotational temperature calculated from this and several other pairs of lines (R(10),P(3); R(38),P(31); R(43),P(36); R(46),P(39)) ranged from 260 to 350 K. Each temperature measurement was an average of 3 to 7 scans over the same two rotational lines during a run, which yielded an estimated standard deviation of 20 to 30 K. The IF(X) generated as a function of $F_2$ flow rate is shown in Fig. 14.

## 4.3 VARIATION OF COMBUSTOR PARAMETERS

Iodine consumption was examined as a function of a number of device parameters including diluent mole fraction, diluent type, $F_2$:NO stoichiometry, combustor pressure (flow rate), and combustor geometry. The latter was modified by installing a choking throat (0.048-in horizontal slit) approximately halfway through the combustor section. Although $N_2$,

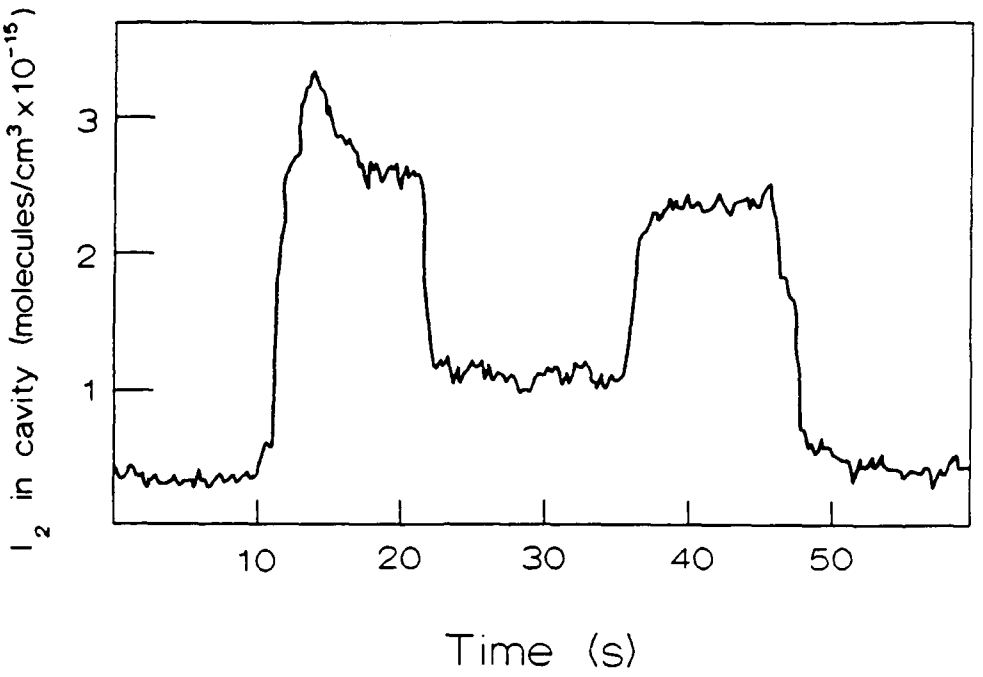


Figure 12. Typical iodine absorption profile in the nozzle cavity during a run. The stoichiometry was $F_2$:NO:$N_2$ = 1:1:5 and the optional throat was not present.

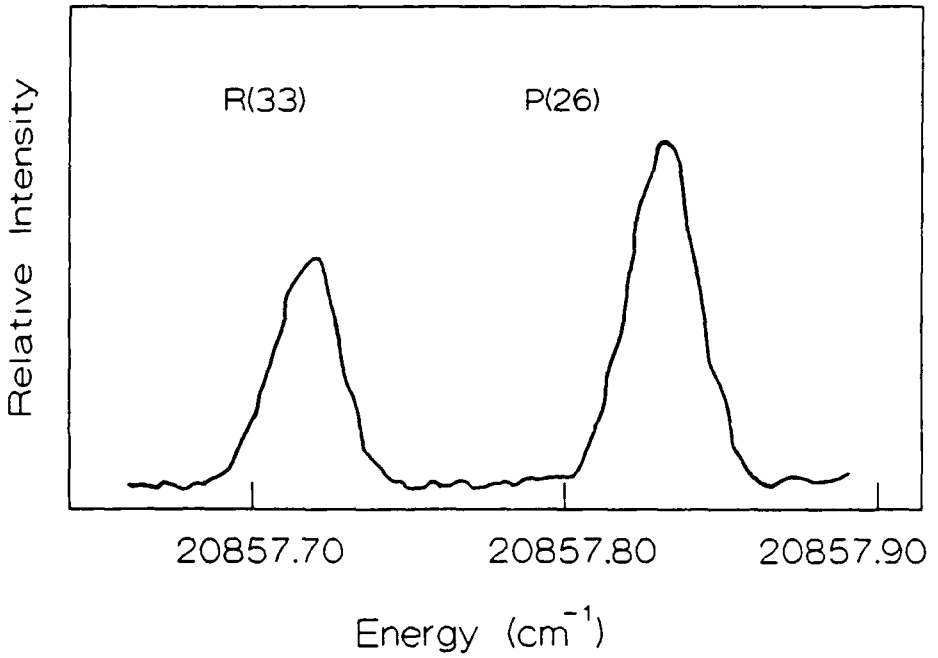


Figure 13. R(33) and P(26) rotational absorption transitions of the IF(X,$v''$=0MB,$v'$=5) band.

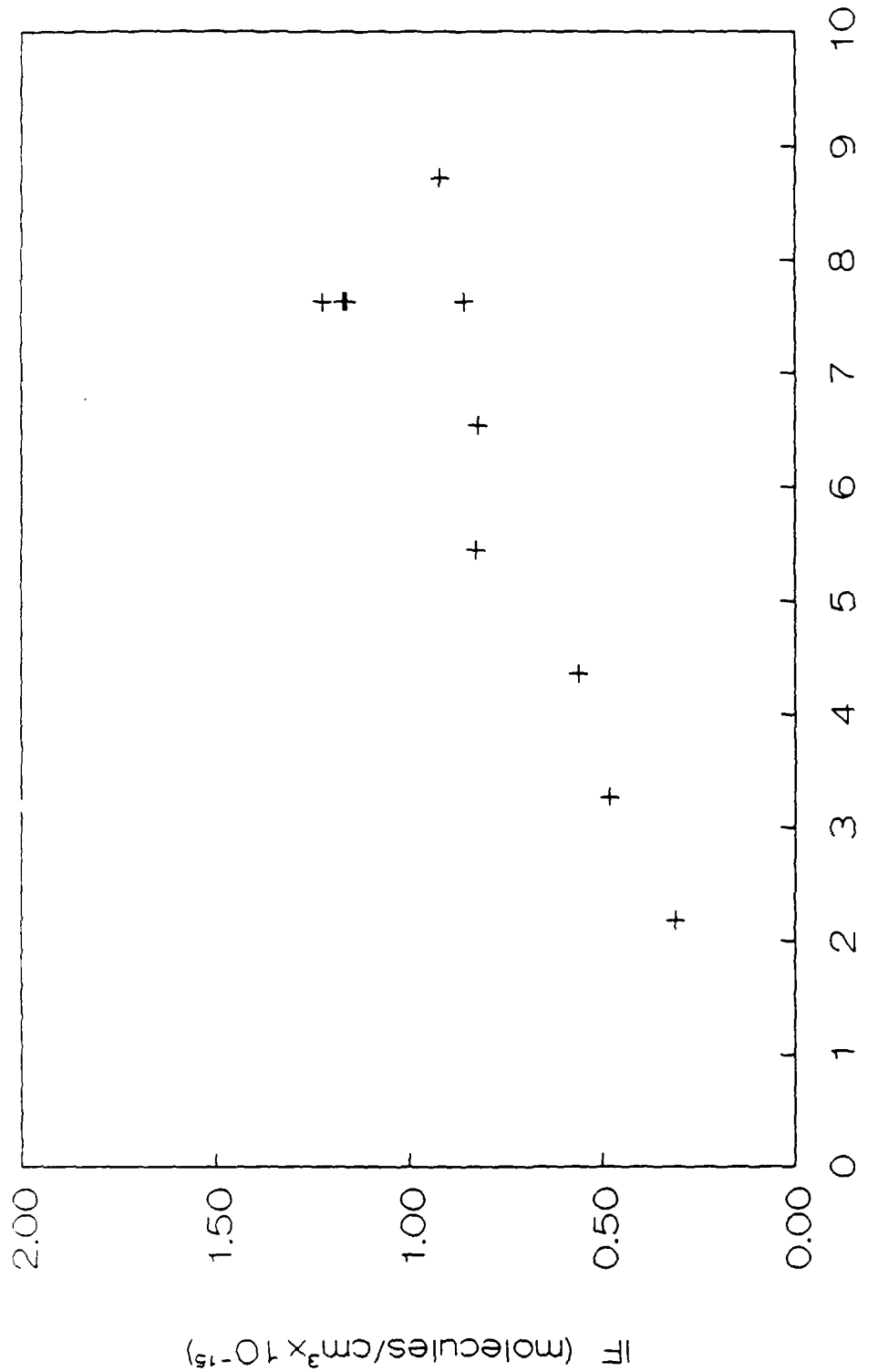


Figure 14. IF(X,v" = 0) number density in the nozzle cavity versus $F_2$ flow rate ($F_2$:NO:$N_2$ = 1:1:5).

Ar, and He each served as diluent in the flowtube, all of the data presented here were collected using nitrogen. The $F_2$:NO:$N_2$ stoichiometry was varied from 1:1:2 to 1:1:15. Although the low diluent conditions produced considerably elevated combustor temperatures, no significant effect on the combustor efficiency (defined as F atoms out/$F_2$ in) was observed. In addition, the combustor efficiency was only weakly dependent on combustor pressure, as shown in Fig. 15. Installation of the choking throat in the combustor permitted the residence time and pressure to be increased to study the changes in combustor performance. Surprisingly similar efficiency results were obtained with and without this additional flow restriction. The combustor temperature profiles, however, were strongly dependent on the presence of the throat. The combustor temperature was monitored at 5 cm and 11 cm downstream of the triplet injector, on opposite sides of the optional throat. Without the throat, the downstream temperature (150 to 250°C) was higher than the upstream temperature (50 to 100°C). With the restriction, the downstream temperature (150 to 200°C) was considerably lower than the upstream temperature (250 to 300°C). Finally the $F_2$:NO stoichiometry was examined to maximize F atom yield (Fig. 16). A slight excess of NO yielded the best results, but clearly the optimal stoichiometry does not deviate appreciably from $F_2$:NO = 1:1.

A bright yellow flame (≈ 1 cm long) was observed immediately downstream of the iodine injectors when all flows were on. This emission was recorded using an OMA I detection system. Approximately 30 bands were resolved from 500 to 700 nm, which were assigned as vibrational bands of the IF(B→X) system. A vibrational temperature of 1100 to 1200 K was extracted from the emission spectrum. This temperature is in fairly good agreement with the results of Whitehead (Ref. 11).

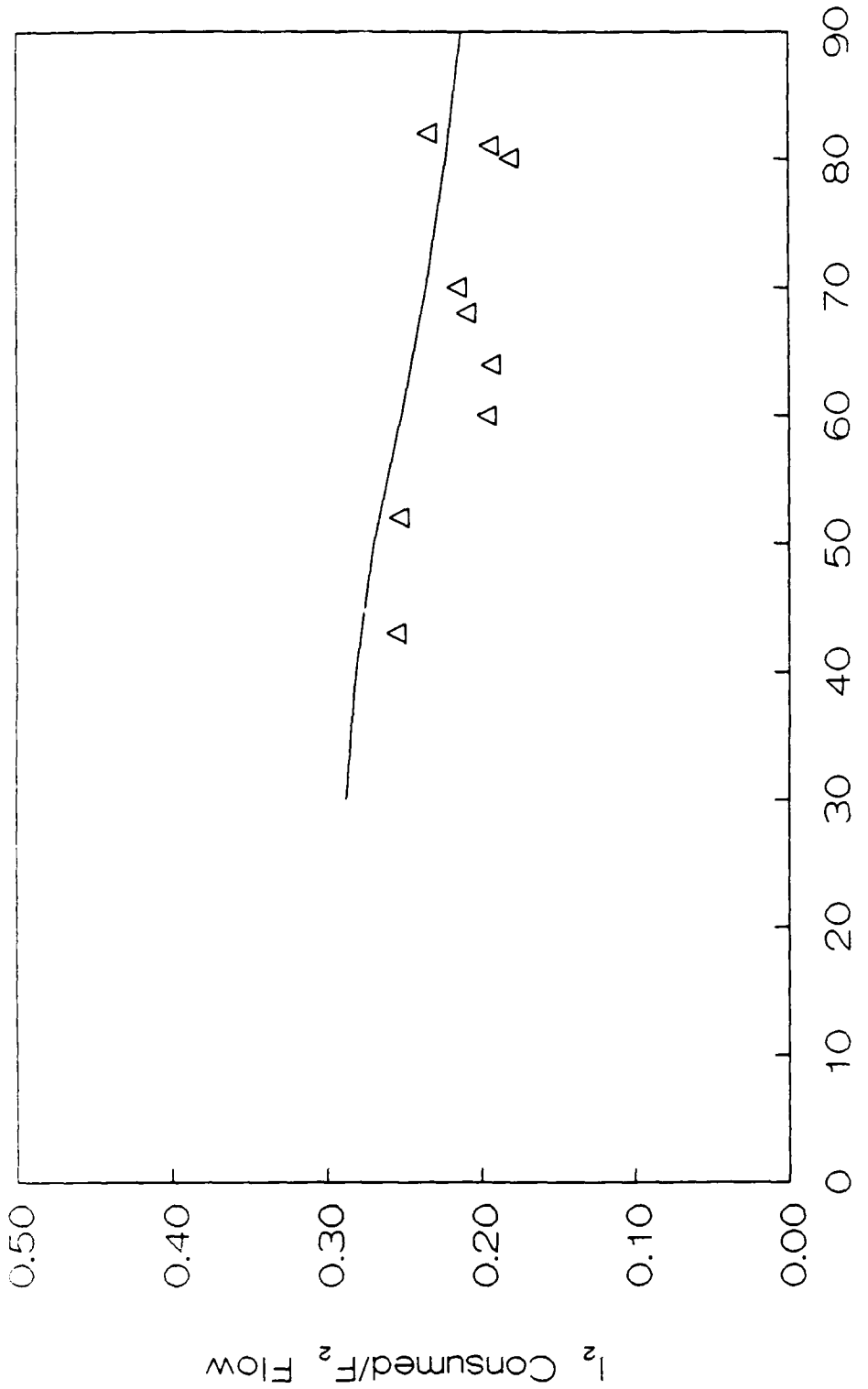


Figure 15. Iodine consumed/$F_2$ delivery versus combustor pressure with $F_2$:NO:$N_2$ = 1:1:5. The solid line is the prediction of the model.

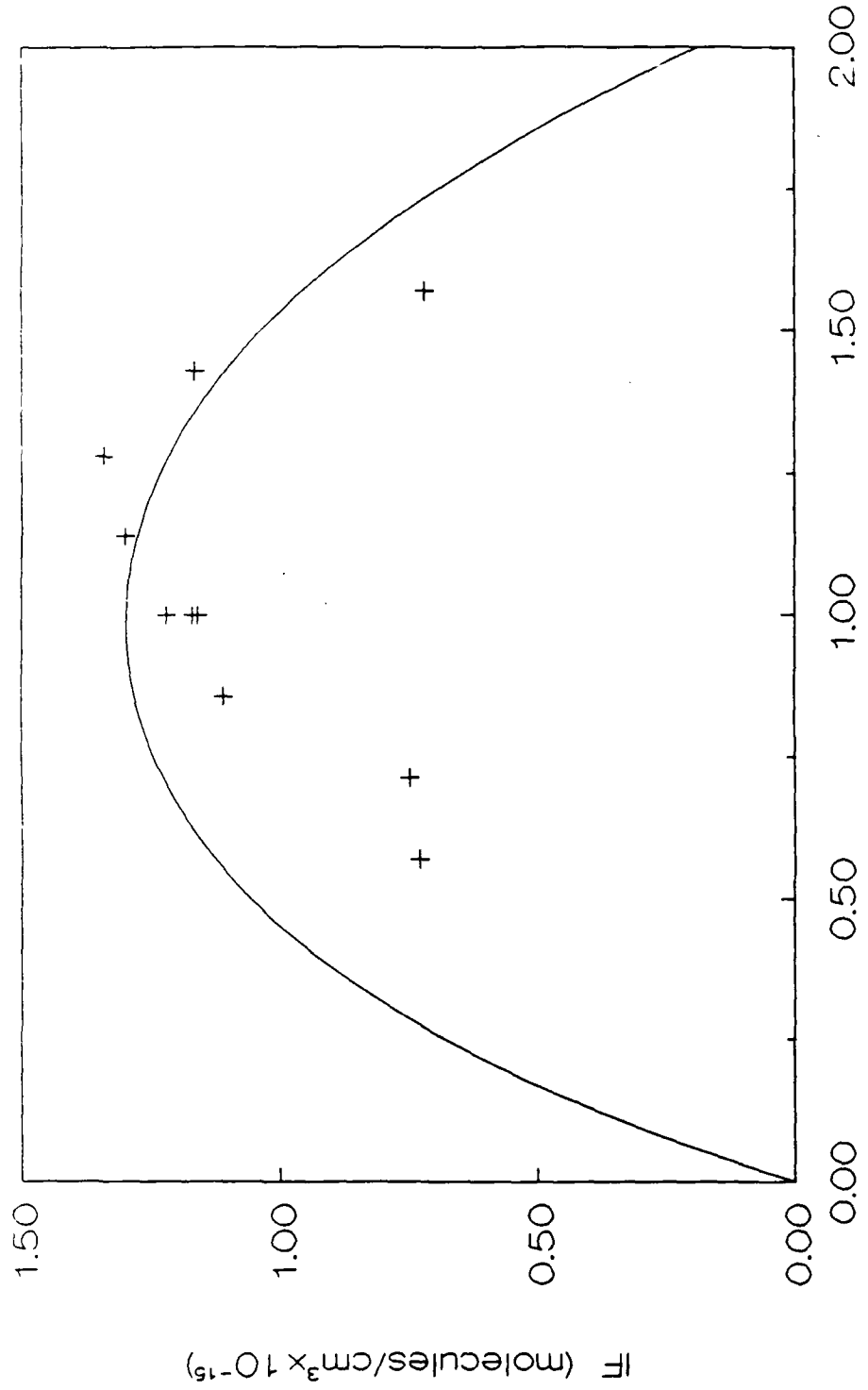


Figure 16. IF(X,v" = 0) number density in the nozzle cavity as a function of $F_2$:NO stoichiometry. The $F_2$ flow was held constant at 7.6 mmol/s. The optional throat was not present and total $N_2$ flow through the combustor was fixed at 38 mmol/s. The solid line is the prediction of the model.

# 5.0 DISCUSSION

## 5.1 COMPARISON OF $I_2$ REMOVAL AND IF PRODUCTION

Most of the data concerning combustor performance were obtained using $I_2$ removal as the critical diagnostic tool. Therefore, it is important to establish a correlation between $I_2$ removal and IF(X) production. This interpretation of the data assumes that $F + I_2 \longrightarrow IF(X) + I$ is the only important path for the loss of $I_2$. Unfortunately, no simultaneous comparison of $I_2$ removal and IF production was possible because of the diagnostic setup used. However, the total $I_2$ delivery can be compared to IF production. The fraction of the $I_2$ delivered that appeared as IF(X,$v''$ = 0) is shown in Fig. 17 as a function of fluorine flow rate. The flattening of this curve is interpreted as complete $I_2$ removal. Approximately 30 percent of the $I_2$ removed does not appear in the IF(X,$v''$ = 0) absorption measurement. There are several possible sources for this discrepancy. One, there may be small amounts of IF in other vibrational levels of IF(X) below the detection limit, or even in the metastable IF(A) state. Two, some process may remove IF before it is measured. However, IF(X,$v''$ = 0) was measured at several positions and no measureable differences were observed. Three, $I_2$ may be removed by some reaction other than $F + I_2$. No known rate coefficients for reactions expected to occur in the cavity compare with the $F + I_2$ coefficient of ($4.3 \times 10^{-10}$) (Ref. 7). The $I(^2P_{1/2}) + I_2$ rate is quite fast, but the $I(^2P_{1/2})$ produced by $F + I_2$ is reported to be negligible (Ref. 6). The authors are not aware of any measured rates for $FNO + I_2$, but it is probably not important for the following reason. When the combustor is operated NO rich ($F_2$:NO = 1:2), $I_2$ removal is greatly diminished. If $FNO + I_2$ could compete with $F + I_2$, then much more $I_2$ should be consumed under NO rich conditions than was observed. (4) Some systematic error(s) may also be responsible for the discrepancy. At any rate, the $I_2$ removal is almost certainly caused by the presence of F atoms, and thus $I_2$ removal is a better measure of combustor performance (F atoms out/$F_2$ in) than the measured IF(X) concentration.

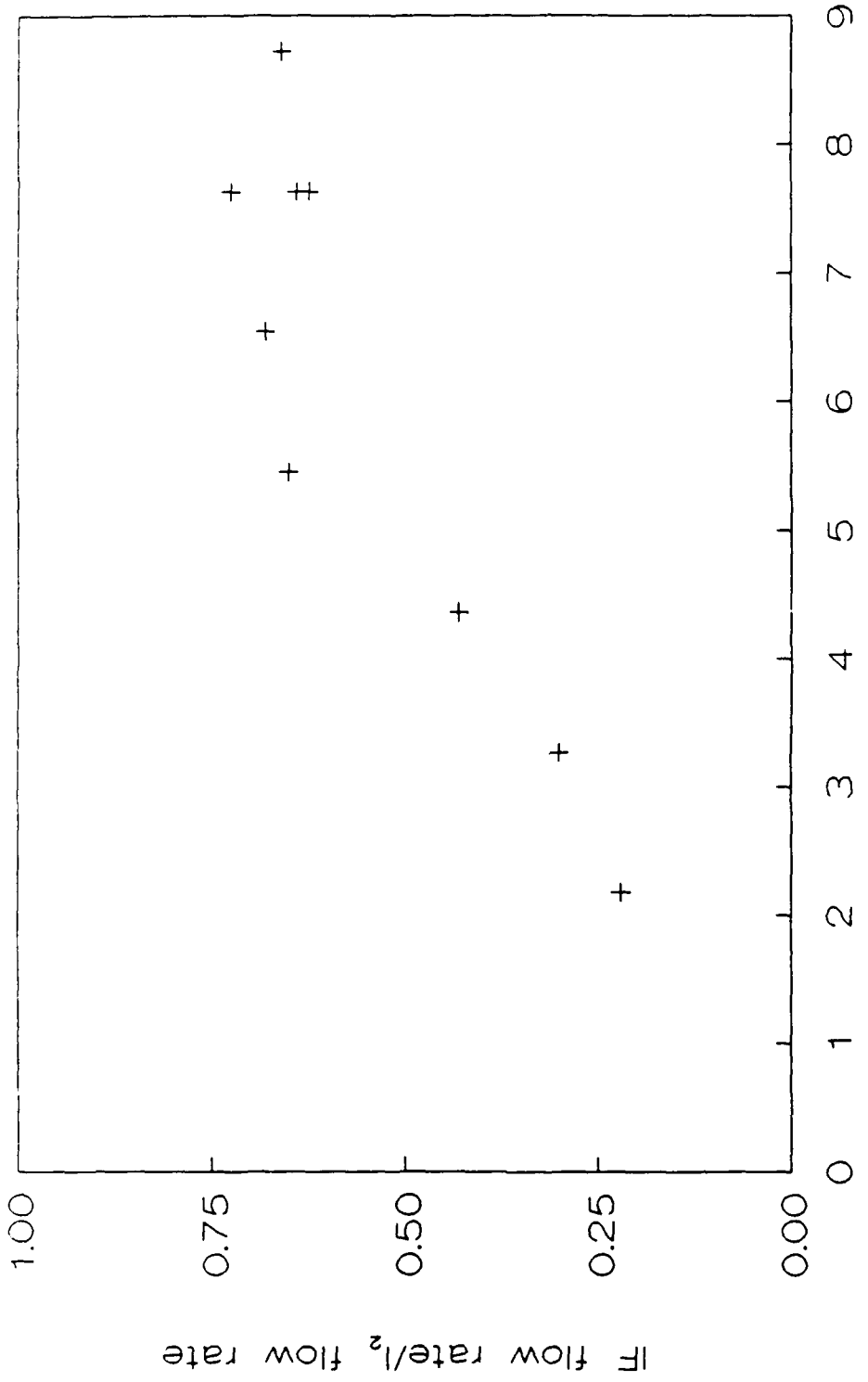


Figure 17. Fraction of iodine delivery that appears as IF(X,$v''$=0) versus fluorine flow rate. Optional throat not present and $F_2$:NO:$N_2$ = 1:1:5.

## 5.2 MODELING OF COMBUSTOR PERFORMANCE

The behavior of the NO\$F_2$ combustor as a function of device conditions was unanticipated. A simple one-dimensional, constant pressure numerical model of the combustor was developed to rationalize the experimental results. Differential equations for specie and energy conservation, including chemical reaction, were numerically integrated with a second-order Runge-Kutta routine using the ideal gas equation of state. Instead of solving the momentum equation, experimentally determined flow rates, pressures, and temperatures were used to derive gas flow velocities. For simplicity, only three reactions were included:

(1) $NO + F_2 \xrightarrow{k_1} FNO + F$ $\quad k_1(T)=7\times10^{-13}e^{-1150/T}cm^3/molecule\text{-}s$ (Ref. 12)

(2) $NO + F + M \xrightarrow{k_2} FNO + M$ $\quad k_2 = 1.1\times10^{-31}cm^6/molecule^2\text{-}s$ (Ref. 13)

(3) $F + F + M \xrightarrow{k_3} F_2 + M$ $\quad k_3 = 5.5\times10^{-34}cm^6/molecule^2\text{-}s$ (Ref. 14)

The third body (M) is an arbitrary collision partner, predominantly the nitrogen buffer gas. Recombination of F atoms on the walls was neglected. Heat transfer to the walls and mixing time were included as parameters. Linear scheduled mixing was used to model the introduction of reactants to the combustor. These two parameters were used in an attempt to reproduce the data in Figs. 15 and 16 and the temperatures from two thermocouples located 5 and 11 cm downstream of the NO and $F_2$ injectors.

With a single set of parameters for heat transfer and mixing time, the model successfully reproduced all the major trends in the data. Specifically, the F atom production efficiency predicted by the model matched the measured efficiency (20 to 30 percent) within experimental error. This value is primarily controlled by the partitioning of NO between reactions (1) and (2). Furthermore, the model predicts the efficiency to be rather insensitive to combustor operating conditions, as shown in Fig. 15. The F atom efficiency data were best fit with a rate coefficient ($k_2 = 1.4\times10^{-31}$ $cm^6/molecule^2$-s) for reaction (2). This rate coefficient includes the effects of both nitrogen and nitric oxide as M in

the recombination process. Using the reported (Ref. 15) rate coefficients for $k_2(M = N_2) = 1.1 \times 10^{-31}$ $cm^6/molecule^2$-s and $k_2(M = NO) = 1.7 \times 10^{-31}$ $cm^6/molecule^2$-s and assuming the concentration of NO is given by its initial unreacted value, a net rate coefficient of $k_2 = 1.4 \times 10^{-31}$ $cm^6/molecule^2$-s is obtained for the $F_2$:NO:$N_2$ = 1:1:5 stoichiometry. The current results for F atom efficiency also agree quite well with a previous predictio· of 18 percent (Ref. 16).

The modeling has led to three conclusions concerning the performance of the combustor: (1) mixing of the NO and $F_2$ streams is poor but complete after 10 cm, (2) heat transfer to the walls is significant, with a heat transfer coefficient h = 0.0016 $cal/cm^2 \cdot s \cdot K$, and (3) once the NO is consumed, F atom losses are minimal. Reactions (1) and (2) must be assumed to rationalize the temperature data and reaction (3) must be assumed to match the observed F atom efficiency.

The model also adequately predicts the dependence of combustor performance on $F_2$:NO stoichiometry, as shown in Fig. 16. In order to compare the trends in the data and the model in Fig. 16, the predicted values for the concentration of F atoms delivered to the nozzle throat were normalized to the observed IF concentration at $F_2$:NO = 1:1. The combustor performance is nearly independent of stoichiometry in the range $F_2$:NO = 1:0.75-1:1.25. The maximum F atom yield is achieved when the $F_2$:NO stoichiometry is adjusted so that the NO is exhausted just as the rate of reaction (2) reaches the rate of reaction (1). Under these experimental conditions, where $F_{out}/F_2(in) \approx 0.2$, $T \approx 550$ K, and $k_2[M]/k_1 \approx 2$, the model and the data indicate that the NO is equally likely to react with both $F_2$ and F at $F_2$:NO ≈ 1:1.

## 5.3 CORRECTION TO IF ABSORPTION CROSS SECTION

Iodine monofluoride number densities were calculated using the absorption cross section given by Clyne for a rotational transition (Ref. 17):

$$\sigma = \frac{8\pi^3}{3hc}\left[\frac{4\ln 2}{\pi}\right]^{1/2}\left[\frac{\nu_o}{\Delta\nu_D}\right]|R_e|^2 \times \frac{S_J F_{vib} F_{rot} q_{v',v''}}{(2J+1)} \qquad (1)$$

where $\nu_o$ is line center, $R_e$ is the transition moment, $S_J/(2J+1)$ is the rotational line strength, $F_{vib}$ and $F_{rot}$ represent the fraction of the ensemble having given v and J values, $q_{v',v''}$ is the Franck-Condon factor for the transition, and $\Delta\nu_D$ is the full-width half-maximum (FWHM) of the absorption band, which is assumed to be Doppler broadened. Clyne assumed $\Delta\nu_D$ = 600 MHz, which corresponds to a 300-K Doppler temperature (Ref. 18). Davis, et al (Ref. 8) measured the width of one rovibronic transition in IF(X→B) to be 1200 MHz under Doppler broadened conditions at room temperature. They attributed the additional broadening to hyperfine splitting from coupling the iodine atom nuclear spin with the rotational angular momentum of IF. A $\Delta\nu_D$= 1200 MHz was also observed in the present study, and used in Equation 1 to determine the IF(X) number densities. This correction is valid to the extent that the line shape is still Gaussian and cross-relaxation among the hyperfine levels is fast. Using Equation 1, $\sigma = 2.7 \times 10^{-17}$ cm$^2$ is calculated for the R(33) line of IF(X,$v''$ = 0⟶B,$v'$ = 5) at 300 K.

The IF formation was extremely rapid, indicating that the mixing of the $I_2$ into the combustor exit flow was good. The IF(X) flow measured 1 to 2 mm downstream of the large $I_2$ injection holes was the same as all other downstream positions, within experimental error. This corresponds to a complete mixing time of ≈10 $\mu$s. Also, the IF(X) flow measured 20 cm (≈0.3 ms) downstream of the $I_2$ injectors matched that measured at 5 cm downstream. The decomposition of IF into $IF_5$ and $I_2$ reported elsewhere (Ref. 7) is apparently not a problem under these operating conditions.

The presence of IF(X, $v'' \geq 8$) is thought to be crucial to the excitation of IF(X) to IF(B) by $O_2(^1\Delta)$ (Ref. 6). The F + $I_2$ reaction was chosen as the IF source in part because a large fraction of the IF(X) produced has $v'' \geq 8$ (Ref. 6). The failure to detect any IF(X,$v''$>0) is not necessarily contradictory to Davis' claim (Ref. 6). The flow conditions at the point of IF production in the present study (40 torr, Mach 0.5) were not conducive to preserving the nascent vibrational distribution of IF(X). In fact, the vibrational relaxation rate suggested by Davis et al predicts that IF(X,$v''\geq 8$) could not be seen under these conditions. Future experiments that couple IF(X) production to $O_2(^1\Delta)$ excitation will be

designed to preserve the initial vibrational distribution of IF(X) long enough to allow excitation by $O_2(^1\Delta)$.

# 6.0 CONCLUSIONS

Ground state IF has been produced in number densities in excess of $10^{15}$/cc in a low pressure flow. Iodine monofluoride was generated by the F + $I_2$ reaction, whereas F was produced by the reaction of NO with $F_2$. The efficiency at the combustor was independent of flow conditions and is adequately modeled with existing kinetic data. The flow environment is relatively clean, and the pressures (3 torr) and temperatures (≈300 K) are suitable for lasing. Ground state IF was observed to be rotationally thermalized (260 to 350 K), and the absence of absorption from IF(X,v"$>$0) indicates a low (probably 300 K) vibrational temperature.

The demonstration of high number densities of IF(X) in a low-pressure flow is an important step toward attempting an IF(B-X) visible chemical laser. Planning is now under way to couple the existing flowtube to a $O_2(^1\Delta)$ generator to study the production of IF(B) under these high number density conditions.

## REFERENCES


1. Davis, S.J., "Prospects for Visible Chemical Lasers," Proc. SPIE 540 p. 188, 1985.

2. McDermott, W.E., Pchelkin, N.R., Benard, D.J., and Bousek, R.R., "An Electronic Transition Chemical Laser," Appl. Phys. Lett. 32 p. 469, 1978.

3. Davis, S.J., Hanko, L., and Shea, R.F., "Iodine Monofluoride $B^3\Pi\ (0^+) \rightarrow X\ ^1\Sigma^+$ Lasing from Collisionally Pumped States," J. Chem. Phys. 78, p. 172, 1983.

4. Whitefield, P.D., Shea, R.F., and Davis, S.J., "Singlet Molecular Oxygen Pumping of IF $B^3\Pi(0^+)$," J. Chem. Phys. 78, p. 6793, 1983.

5. Piper, L.G., Marinelli, W.J., Rawlins, W.T., and Green, B.D., "The Excitation of IF $B(^3\Pi_o)$ by $N_2$ $A(^3\Sigma_u^+)$," J. Chem. Phys. 83, p. 5602, 1985.

6. Davis, S.J., Woodward, A.M., Piper L.G., and Marinelli, W.J., "Chemical Pump Sources for IF(B)," PSI-2000/TR-689, Physical Sciences Inc., Research Park, P.O. Box 3100, Andover, MA 01810, June 1987.

7. Appelman, E.H. and Clyne, M.A.A., "Reaction Kinetics of Ground State Fluorine, F $^2P$ Atoms," J.C.S. Faraday I 71, p. 2072, 1975.

8. Davis, S.J., Hanko L., and Wolf, P.J., "Continuous Wave Optically Pumped Iodine Monofluoride $B^3\Pi(0^+) \rightarrow X\ ^1\Sigma^+$ Laser," J. Chem. Phys. 82, p. 4831, 1985.

9. Davis, S.J., and Hanko, L., "Optically Pumped Iodine Monofluoride $B^3\Pi(0^+) \rightarrow X^1\Sigma^+$," Appl. Phys. Lett. 37, p. 692, 1980.

10. Cool, T.A. and Stephens, R.R., "Chemical Laser by Fluid Mixing," J. Chem. Phys. 31, p. 5175, 1969.

11. Raybone, D., Watkinson, T.M., and Whitehead, J.C., "The Production of Long-Lived IF($B^3\Pi$) Emission in the 248 nm Photolysis of a Mixture of $CF_3I$ and $F_2$," Chem. Phys. Letters 135, p. 170, 1987.

12. Kolb, C.E., "Reactions of Fluorine Atoms," J. Chem. Phys. 64, p. 3087, 1976.

13. Skolnik, E.G., Veysey, S.W., Ahmed, M.G., and Jones, W.E., "Rate Constants for the Reaction of Fluorine Atoms with Nitric Oxide in the Presence of Various Third Bodies," Can. J. Chem. 53, p. 3188, 1975.

14. Ultee, C.J., "The Homogeneous Recombination Rate Constant of F Atoms at Room Temperature," J. Chem. Phys. 46, p. 366, 1977.

15. Kim, P., Maclean, D.I., and Valance, W.G., "Reaction Kinetics of Nitric Oxide with F and with $F_2$ by ESR Spectroscopy," Paper No. FRK-122, Power Branch, Office of Naval Res., 1972.

16. Hoell, J.M., Jr., Allario, F., Jarrett, O., Jr., and Seals, R.K., Jr., "Measurements of $F_2$, NO, and ONF Raman Cross Sections and Depolarization Ratios for Diagnostics in Chemical Lasers," J. Chem. Phys. 38, p. 2896, 1973.

17. Clyne, M.A.A., and McDermid, I.S., "Quantum-Resolved Dynamics of Excited States Part 4.- Radiative and Predissociative Lifetimes of IF $B^3\Pi(0^+)$," J. Chem. Soc. Faraday Trans II 74, p. 1644, 1977.

18. Demtröder, W., Laser Spectroscopy, p 87, Springer-Verlag, New York, NY, 1982.

# APPENDIX

## SELECTED ENGINEERING DRAWINGS FOR DEVICE HARDWARE

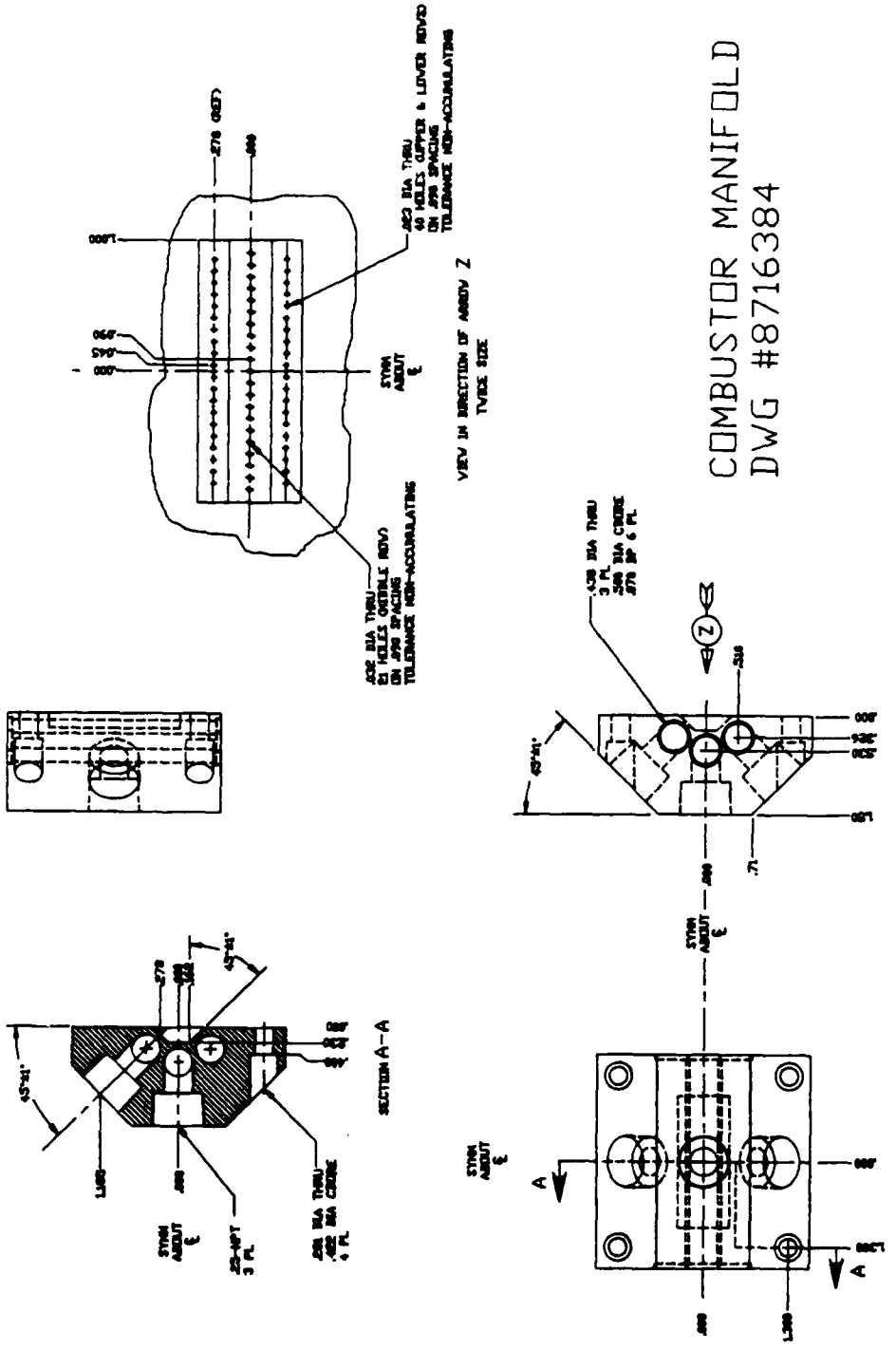
COMBUSTOR MANIFOLD
DWG #8716384
SECTION A-A
VIEW IN DIRECTION OF ARROW Z

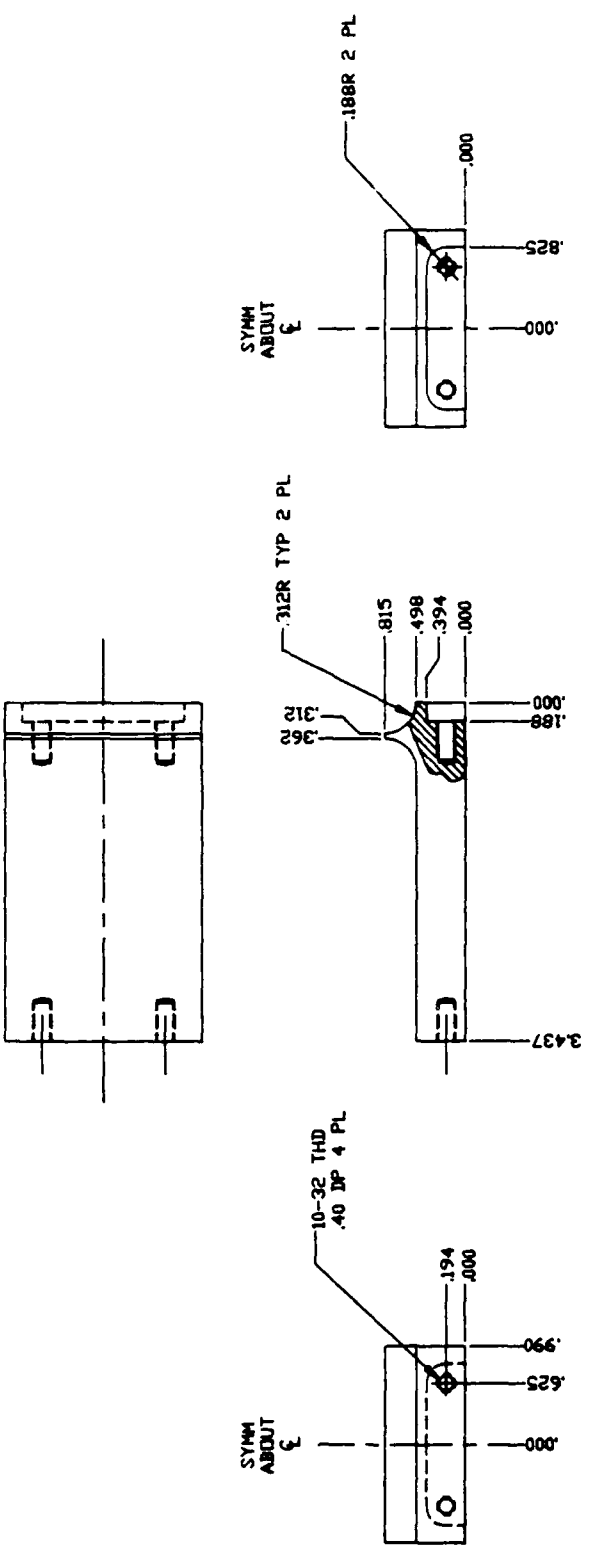


OPTIONAL COMBUSTOR BLADE
DWG #8716386

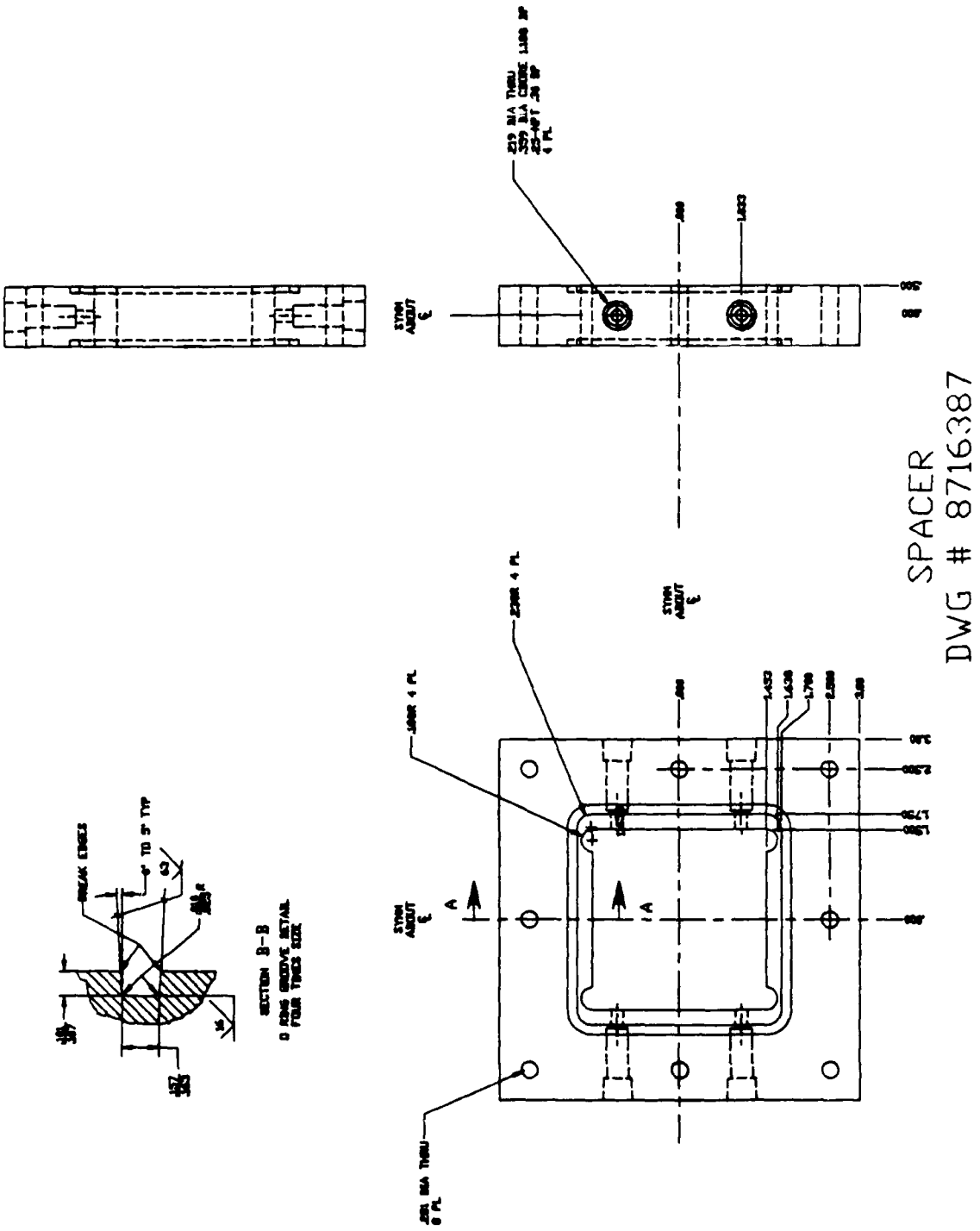

SPACER
DWG # 8716387

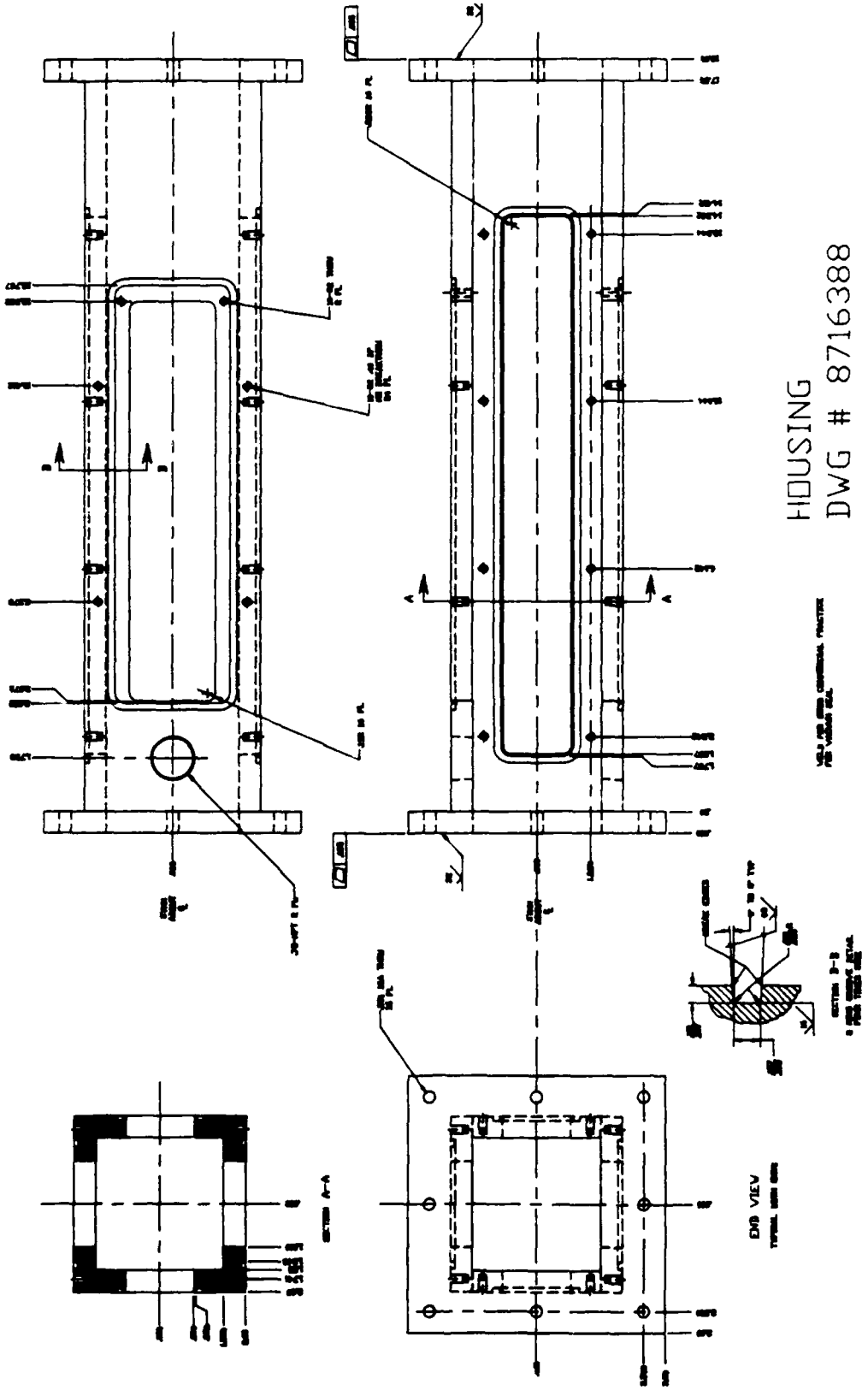

HOUSING
DWG # 8716388

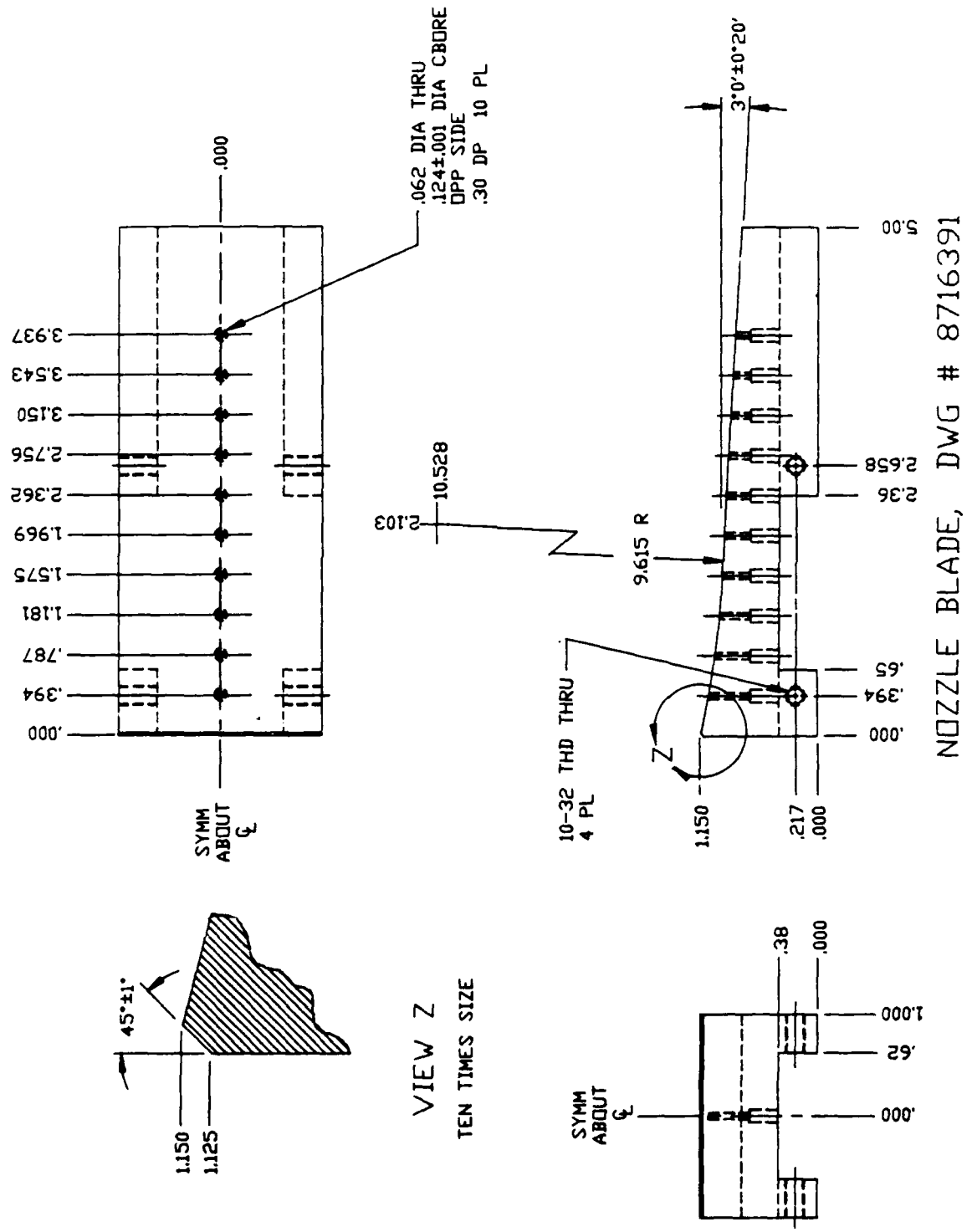
NOZZLE BLADE, DWG # 8716391
.062 DIA THRU
.124±.001 DIA CBORE
OPP SIDE
.30 DP 10 PL
3°0'±0°20'
5.00
2.658
2.36
.65
.394
.000
9.615 R
10.528
2.103
10-32 THD THRU
4 PL
Z
1.150
.217
.000
SYMM
ABOUT
℄
3.937
3.543
3.150
2.756
2.362
1.969
1.575
1.181
.787
.394
.000
45°±1°
1.150
1.125
VIEW Z
TEN TIMES SIZE
.38
.000
1.000
.62
.000
SYMM
ABOUT
℄

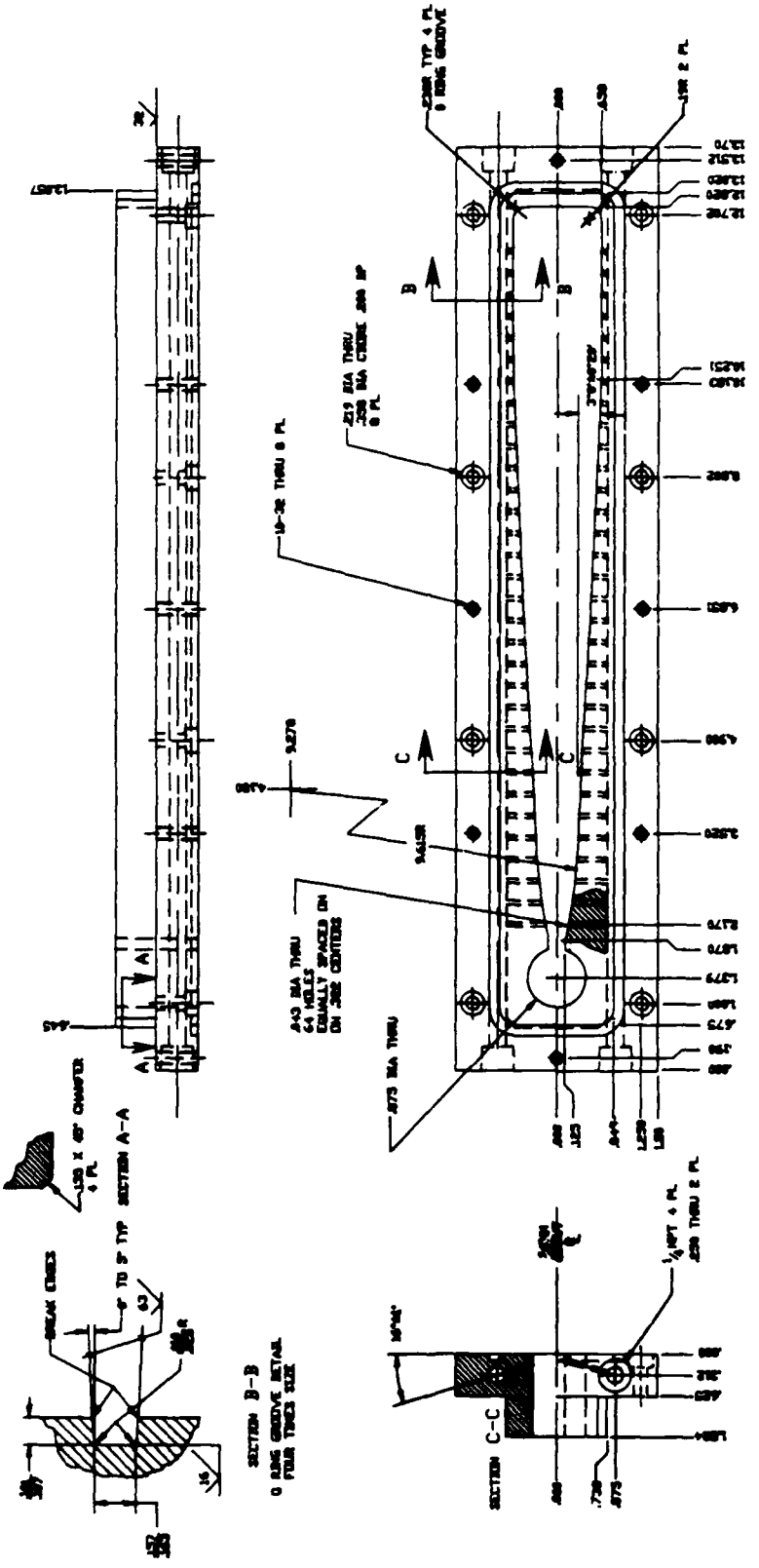

OUTER SIDE PLATE
DWG. #8716393

(This page intentionally left blank.)

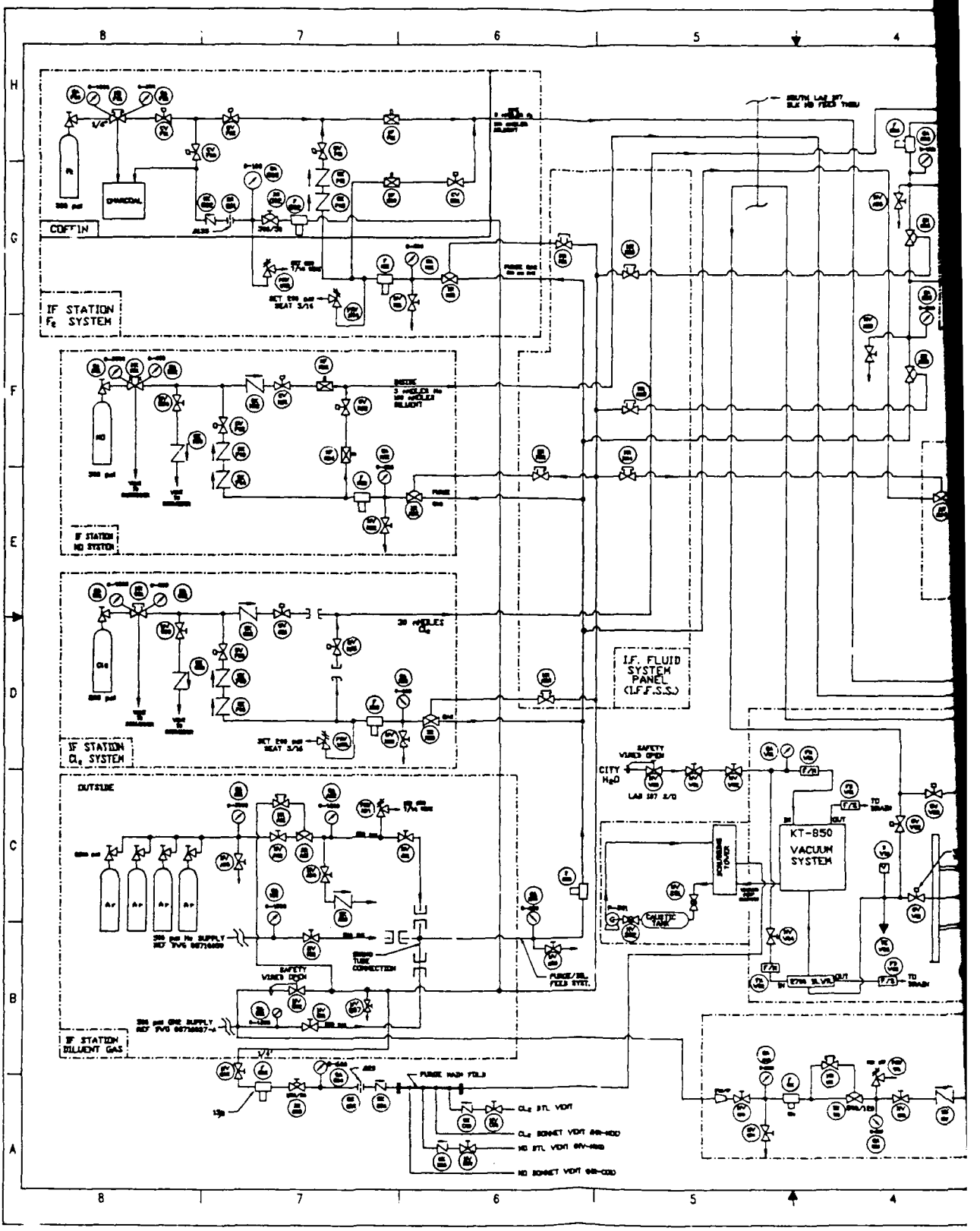
COFFIN
IF STATION $F_e$ SYSTEM
IF STATION $N_i$ SYSTEM
IF STATION $Cl_2$ SYSTEM
OUTSIDE
IF STATION DILUENT GAS
I.F. FLUID SYSTEM PANEL (I.F.F.S.S.)
KT-850 VACUUM SYSTEM
CITY $H_2O$
SAFETY VALVES OPEN
SAFETY VALVES CLOSED
PURGE/SEL FIELD SYST.
PURGE MAIN FEED
TO DRAIN

162

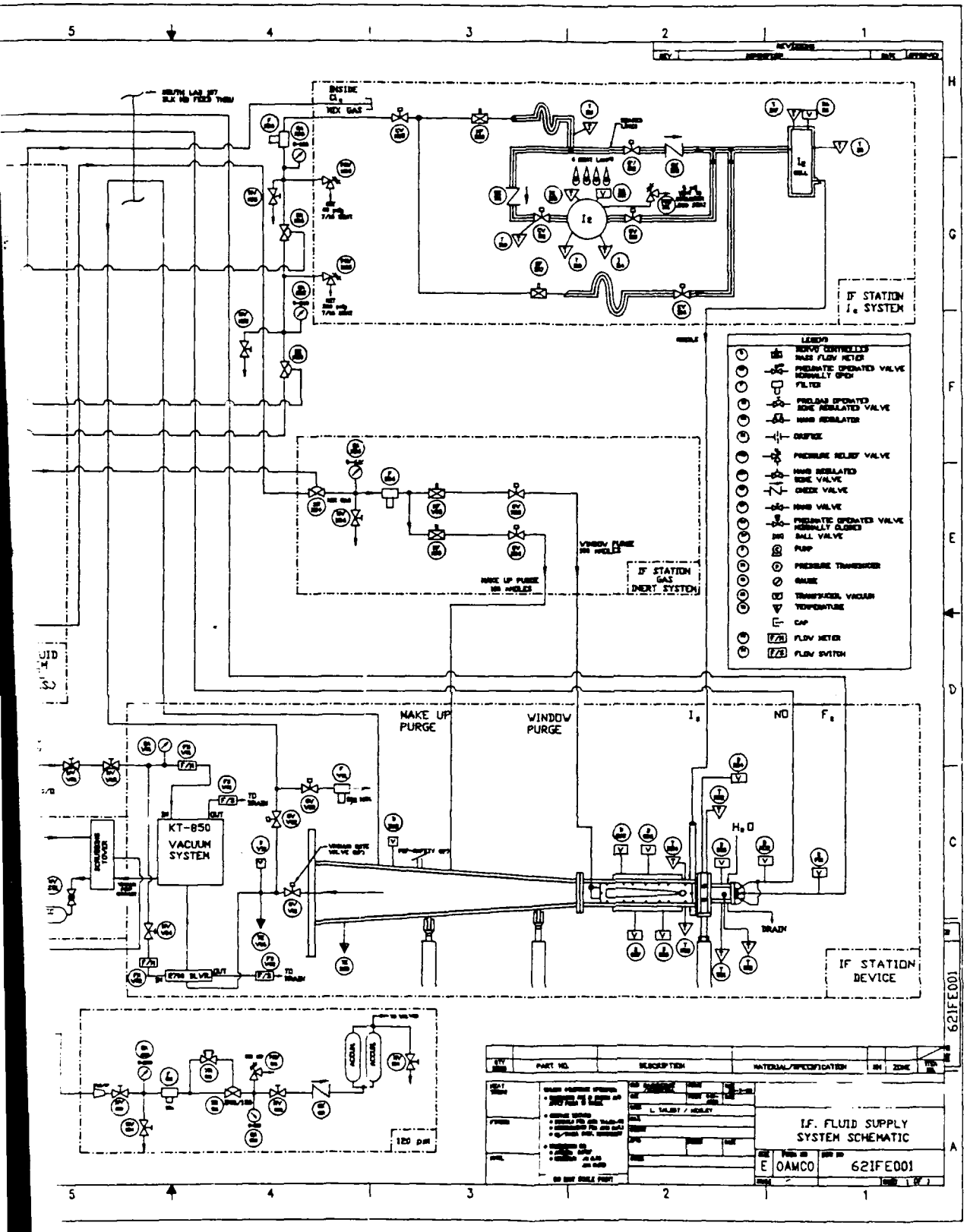
IF STATION
SYSTEM
IF STATION
GAS
INERT SYSTEM
MAKE UP
PURGE
WINDOW
PURGE
NO
KT-850
VACUUM
SYSTEM
IF STATION
DEVICE
I.F. FLUID SUPPLY
SYSTEM SCHEMATIC
E
OAMCO
621FE001



2012